NASA TECHNICAL MEMORANDUM

NASA TM X- 62,245

NASA TM X- 62,245

COMPUTER SIMULATION OF AIRCRAFT MOTIONS AND PROPULSION SYSTEM DYNAMICS FOR THE YF-12 AIRCRAFT AT SUPERSONIC CRUISE CONDITIONS

Stuart C. Brown

Ames Research Center
Moffett Field, Calif. 94035

August 1973

COMPUTER SIMULATION OF AIRCRAFT MOTIONS AND PROPULSION SYSTEM DYNAMICS FOR THE YF-12 AIRCRAFT AT SUPERSONIC CRUISE CONDITIONS

Stuart C. Brown

Ames Research Center

SUMMARY

This report describes a computer simulation of the YF-12 aircraft motions and propulsion system dynamics. The aircraft is a delta-wing twin-engine type which is capable of cruising at high altitudes and supersonic Mach numbers and the simulation is intended to represent the aircraft and its systems for these conditions. The propulsion system was represented in sufficient detail so that interactions between aircraft motions and the propulsion system dynamics could be investigated.

Six degree-of-freedom aircraft motions together with the three-axis stability augmentation system were represented. The mixed compression inlets and their controls were represented in the started mode for a range of flow conditions up to the inlet unstart boundary. Effects of inlet moving geometry on aircraft forces and movements as well as effects of aircraft motions on the inlet behavior were simulated. The engines, which are straight turbojets, were represented in the afterburning mode, with effects of changes in aircraft flight conditions included. The simulation was capable of operating in real time.

INTRODUCTION

One portion of the overall NASA YF-12 research program is directed toward investigations of interactions between aircraft motions and elements of the propulsion system during high-altitude supersonic cruise conditions. The program includes flight test, wind tunnel, and control investigations. These interactions become of increased importance for aircraft with mixed-compression inlets such as those used on the YF-12. While the mixed-compression inlet is the most efficient type for Mach numbers greater than about 2.2, the inlet is quite sensitive to aircraft motions and the resulting flow changes. Furthermore, precise control of its moving geometry is required to achieve this design efficiency. This report describes a digital computer simulation which was prepared for the investigation of these interaction problems. The simulation was intended to be used for two purposes. The first was for comparisons of predicted with flight test results, while the second was for developing control systems which would reduce the interactions to suitably small levels.

The simulation was developed for overall representations of the aircraft motions and propulsion system dynamics for cruise conditions at high altitude (above 15.24 km) and supersonic Mach numbers (greater than about 2.4). Six degree-of-freedom aircraft motions together with the three-axis stability augmentation system were represented. Each inlet, operating in the started mode, was represented in sufficient detail so that effects of aircraft motions on controlled inlet performance and effects of moving inlet geometry on aircraft motions were included. Each engine was represented in the afterburning mode in a linearized form together with interactions with inlet and aircraft flight condition changes.

The parameter variations for the aircraft motions and engine representations over the flight range of interest were sufficiently moderate so that they could have been stored in the computer over the entire flight range of interest. However, the generation of pertinent inlet flow parameters presented a special problem since the representation of multivariable nonlinear functions was needed.

The use of a tabular form for these functions over the complete range of interest would have required an excessive amount of storage and computation time. In order to facilitate more efficient computer utilization, the simulation was designed to operate only in restricted ranges near selected nominal conditions. Nonlinear functions, principally ones describing inlet parameters, were represented as multivariable power series expansions. These expansions, then depended upon the nominal condition selected. A separate procedure was used to generate the expansion coefficients for selected nominal conditions from available wind tunnel and/or flight data.

NOTATION

A_j	incremental engine primary exhaust nozzle area
a	speed of sound
b	wing span
c	reference wing mean aerodynamic chord
C_D	drag coefficient, $\frac{D}{q_V S}$
C_L	lift coefficient, $\frac{L}{q_V S}$
C_l	rolling-moment coefficient, $\frac{\text{rolling moment}}{q_V Sb}$
C_m	pitching-moment coefficient, $\frac{\text{pitching moment}}{q_V S}$
C_n	yawing-moment coefficient, $\frac{\text{yawing moment}}{q_V Sb}$

C_y	side-force coefficient, $\frac{\text{side force}}{q_v S}$
D	aerodynamic drag
$f_a(\ \ )$	nonlinear function contributing to inlet pressure recovery calculation
$f_b(\ \ )$	nonlinear function contributing to bypass signal pressure calculation
$f_{c_a}(\ \ )$	nonlinear function contributing to airflow unstart boundary calculation
$f_{c_s}(\ \ )$	nonlinear function contributing to spike unstart boundary calculation
g	acceleration due to gravity
h	altitude
I_{xx}, I_{yy}, I_{zz}	rolling, pitching and yawing moments of inertia about body reference axes
I_{xz}	product of inertia about body reference axes
L	aerodynamic lift
M	Mach number
m	aircraft mass
N	incremental engine rotor speed
n_z	normal acceleration at the cg
p,q,r	rolling, pitching and yawing angular velocities about body reference axes
p_s/p_{t_m}	ratio of bypass static pressure signal to free-stream total pressure
p_{t_2}/p_{t_o}	ratio of total pressure at inlet diffuser exit to free-stream total pressure
p_{t_4}/p_{t_o}	ratio of incremental burner total pressure to free-stream total pressure
q_v	dynamic pressure
S	wing area

s	Laplace transform variable
T	time constant
T_t	total temperature
V	nominal forward velocity
w_{e_c}	incremental airflow demanded by the engine corrected to diffuser exit conditions $\dfrac{w_e\sqrt{T_{t_2}/T_{std}}}{p_{t_2}/p_{std}}$
w_{fab}	incremental afterburner fuel flow
w_{fpb}	incremental primary burner fuel flow
X,Y,Z	forces along the x,y,z body axes
x_s	incremental shock wave position from unstart location
α	incremental angle of attack from α_{w_o}
α_w	angle of attack relative to wing reference plane
β	sideslip angle
δ_a	total antisymmetrical elevon deflection
Δw_{i_c}	inlet airflow connected to diffuser exit conditions, $\dfrac{w_i\sqrt{T_{t_2}/T_{std}}}{p_{t_2}/p_{std}}$
Δx	denotes incremental value from the nominal condition, x-xo, for the arbitrary quantity x unless otherwise indicated.
δ_{bp}	position of actuator controlling bypass exit flow
δ_e	symmetrical elevon deflection
δ_r	vertical tail deflection
δ_{sp}	inlet spike position
δ_t	incremental engine thrust
Θ	pitch angle

ρ	mass density of air
ϕ	roll angle

Subscripts

a	total antisymmetrical values of left and right side propulsion system parameters
e	external input
m	measured value
o	nominal value
s	total incremental symmetrical value of left and right side propulsion system parameters
sas	output from stability augmentation system
std	standard value at sea level
2	value at compressor inlet
4	value at primary burner exit

Superscripts

ℓ	left side
r	right side
s	stability axis system

Aerodynamic Derivatives

Generally, derivatives of coefficients are with respect to the indicated subscript; e.g. $C_{n_\beta} \equiv \frac{dC_n}{d\beta}$. An exception to this notation is used for the aerodynamic damping derivatives, C_{l_r}, C_{n_r}, C_{l_p}, C_{n_p}. These terms are derivatives with respect to the subscripts times $\frac{b}{2V}$, e.g. $C_{l_r} = \frac{dC_l}{d(rb/2V)}$.

DESCRIPTION OF AIRCRAFT

The YF-12 is a delta-wing twin-engine aircraft which is capable of cruising at Mach numbers greater than 3 and at altitudes greater than 24.38 km. A three-view drawing of the airplane is shown in figure 1. The aerodynamic controls are as follows. Two elevons on each wing, one inboard and one outboard of each nacelle, operate together symmetrically and antisymmetrically with the pair on the opposite wing to provide longitudinal and lateral control. Two nacelle mounted all-movable vertical tails provide directional control.

The aircraft has two axisymmetric variable geometry, mixed compression inlets. Each inlet has a translating centerbody (spike), which varies the inlet contours with flight condition and a forward bypass door which diverts flow from the engine and dumps it overboard. The forward bypass door is continuously modulated through use of a closed loop control system to maintain the inlet airflow at a desired condition and to prevent inlet unstarts. Mach number as well as angle of attack and sideslip angle signals are supplied to the spike and bypass systems. Other flow is diverted from the inlet by a fixed bleed system on the centerbody which exhausts the flow overboard, a fixed bleed on the cowl, and an aft bypass door. The latter two flows supply secondary air for engine cooling. The aft bypass doors are manually scheduled by preselected increments with flight condition. In the event of an inlet unstart, control signals are scheduled to adjust the inlet spike and forward bypass doors to restart the inlet flow and then return the inlet to its previous position.

The engine is a Pratt and Whitney YJ58 single-spool axial flow turbojet with afterburner. Provision is made to bypass a portion of the air from the compressor. The bypassed air remixes with the primary flow at the entrance to the afterburner. Engine rotor speed is controlled by closed loop adjustment of the exhaust nozzle which varies back pressure on the turbine. The flow exits through a converging-diverging ejector nozzle with adjustable trailing edge flaps. Afterburner fuel flow is an open loop function of power lever angle, burner pressure, and compressor inlet temperature. Primary burner fuel flow depends upon the same quantities plus rotor speed.

DESCRIPTION OF SIMULATION

The purpose of the simulation was to represent both airframe motion and propulsion system dynamics in sufficient detail so that effects of parameter variations and interactions between the systems could be investigated. The simulation was intended for use both for identification with flight test results and for control system studies. Since a simulation which would operate at least as fast as real time was desired, a careful balance was necessary between depth of representation of the various components and computational speed. The simulation was intended to operate in the aircraft motion frequency range, which included the phugoid mode, from about 0.005 to

to 5 hertz. Hence higher frequency effects associated with both aircraft motions and the propulsion system were neglected. Simplifications in the representation of several inlet nonlinear functions, obtained from wind tunnel data, were also necessary. Rather than attempt to represent these functions of several variables in a tabulated form for the complete range of interest, power series expansions, valid for a restricted range, were made relative to selected nominal flight conditions. A procedure for obtaining these functions is discussed in a subsequent section and Appendix A. It was intended that the expansion coefficients be obtained through use of a separate computer program which would curve fit the original data and obtain the coefficients in a form for direct use in the simulation.

The equations used for the simulation are described in detail in the following sections of this report. Descriptions are given of the aircraft, inlet, and engine representations, as well as their respective control systems. Then the numerical integration procedures used are presented. Finally, a listing of the computer program is provided in Appendix B. A sketch of the subsystems represented together with the interconnecting variables for these systems are shown in figure 2. The numerical data used for the simulation are not included in this report.

Airframe Representation

The equations used to obtain six degree-of-freedom rigid-body aircraft motions are given in this section. Effects of inlet and engine forces and moments are included. The representation for the aircraft three-axis stability augmentation system and the control surface dynamics are also described. An outline of the computations performed is shown in figure 3.

Aircraft equations of motion— The following assumptions were made in determining the airframe equations of motion.

1. The airframe is assumed to be a rigid body.

2. The mass of the airplane is assumed to be constant for the portion the flight to be analyzed.

3. The earth is assumed to be flat, nonrotating, and fixed in inertial space.

4. The aircraft has a vertical plane of symmetry.

5. Small angle approximations apply.

Two moving-axis systems were used with origins at the center of gravity of the aircraft. The first is a stability axis system. In the definition used here, the x^S and z^S axes (positive forward and downward respectively) are located in the aircraft plane of symmetry and are aligned parallel and perpendicular to the instantaneous relative wind projected into the plane of

symmetry. The y^s axis is perpendicular to the plane of symmetry (positive to the right). The second axis system is a body axis system which is fixed to the aircraft. The x and y axes are fixed in a wing reference plane (denoted w) which is aligned with the principal wing surface, whereas the z axis is perpendicular to it. The transformation from one axis system to the other is made by a rotation of the angle, α_w, about the common y axis. Aerodynamic stability derivatives and force and moment coefficients were available in the stability axis system. These quantities were transformed to the body axis system and then integrated with the result that motions as measured in flight would be directly represented. Moreover, body motions to be used as SAS signals would also be directly obtained. Since effects of changes in M on stability derivatives are small for the range of interest, they have been neglected.

As part of the initialization procedure, lateral-directional stability derivatives were converted from the stability axis direction to the body axis direction (a rotation of α_{w_o}). The effect of any subsequent changes in α on the lateral-directional stability derivatives was neglected. For these static derivatives, the conversion from stability to body axes was as follows:

$$C_{n_i} = C^s_{n_i} \cos \alpha_{w_o} + C^s_{\ell_i} \sin \alpha_{w_o} \tag{1}$$

$$C_{\ell_i} = C^s_{\ell_i} \cos \alpha_{w_o} - C^s_{n_i} \sin \alpha_{w_o} \tag{2}$$

where the subscript, i, denotes a static derivative such as β, δ_a, etc. For the damping derivatives, the equations for resolving both the moment coefficients and the angular rates from stability to body axes are:

$$C_{n_r} = C^s_{\ell_p} \sin^2 \alpha_{w_o} + C^s_{n_r} \cos^2 \alpha_{w_o} + \left(C^s_{n_p} + C^s_{\ell_r}\right) \sin \alpha_{w_o} \cos \alpha_{w_o} \tag{3}$$

$$C_{\ell_r} = C^s_{n_p} \sin^2 \alpha_{w_o} + C^s_{\ell_r} \cos^2 \alpha_{w_o} + \left(C^s_{\ell_p} - C^s_{n_r}\right) \sin \alpha_{w_o} \cos \alpha_{w_o} \tag{4}$$

$$C_{n_p} = - C^s_{\ell_r} \sin^2 \alpha_{w_o} + C^s_{n_p} \cos^2 \alpha_{w_o} + \left(C^s_{\ell_p} - C^s_{n_r}\right) \sin \alpha_{w_o} \cos \alpha_{w_o} \tag{5}$$

$$C_{\ell_p} = C^s_{n_r} \sin^2 \alpha_{w_o} + C^s_{\ell_p} \cos^2 \alpha_{w_o} - \left(C^s_{n_p} + C^s_{\ell_r}\right) \sin \alpha_{w_o} \cos \alpha_{w_o} \tag{6}$$

where the subscript, s, denotes stability axes and no superscript denotes body axes. The body axis derivatives were used in all subsequent calculations.

Drag and lift forces were initially calculated in the stability axis system.

$$\frac{D^s}{m} = \frac{q_v S}{m}\left[C^s_D(\alpha) + C^s_{D_{\delta_e}} \Delta\delta_e + C^s_{D_{\delta_{bp}}} \delta_{bp_s} + C^s_{D_{\delta_{bp}}} \delta_{sp_s}\right] \tag{7}$$

$$\frac{L^s}{m} = \frac{q_v S}{m}\left[C^s_L(\alpha) + C^s_{L_{\delta_e}} \Delta\delta_e + C^s_{L_{\delta_{bp}}} \delta_{bp_s} + C^s_{L_{\delta_{sp}}} \delta_{sp_s} + \frac{c}{2V} C^s_{L_q} q\right] \tag{8}$$

These forces were subsequently converted to body axis directions in the equations of motion.

The following equations describe the aircraft linear and angular accelerations relative to the body axes.

$$\dot{u} + \alpha_{w_o} Vq = -g\Delta\Theta + X_{\delta_t} \delta_{t_s} - \frac{D^s}{m} + \frac{L^s}{m} \alpha_w + X_o \tag{9}$$

$$\dot{v} + Vr - g \sin \phi - \alpha_{w_o} Vp = \frac{q_{v_o} S}{m}\left(C_{y_\beta} \beta + C_{y_{\delta_r}} \delta_r\right) + \frac{q_{v_o} Sb}{2Vm} C_{y_r} r \tag{10}$$

$$\dot{w} - Vq = Z_{\delta_t} \delta_{t_s} - \frac{D^s}{m} \alpha_w - \frac{L^s}{m} + Z_o \tag{11}$$

$$\dot{p} - \frac{I_{xz}}{I_{xx}} \dot{r} = \frac{q_v Sb}{I_{xx}}\left(C_{\ell_\beta} \beta + C_{\ell_{\alpha\beta}} \alpha\beta + C_{\ell_{\delta_a}} \delta_a + C_{\ell_{\delta_r}} \delta_r + C_{\ell_{\delta_{bp}}} \delta_{bp_a} + C_{\ell_{\delta_{sp}}} \delta_{sp_a}\right) + \frac{q_{v_o} Sb^2}{2VI_{xx}}\left(C_{\ell_r} + C_{\ell_p} p\right) + L_{\delta_t} \delta_{t_a} \tag{12}$$

$$\dot{q} = \frac{q_{v_o} Sc}{2VI_{yy}} \left(C_{m_{\dot{\alpha}}} \dot{\alpha} + C_{m_q} q \right) - \frac{q_{v_o} Sc}{I_{yy}} C_m(0)$$
$$+ \frac{q_v Sc}{I_{yy}} \left(C_m(\alpha) + C_{m_{\delta_e}} \Delta\delta_e + C_{m_{\delta_{bp}}} \delta_{bp_s} \right) + M_{\delta_t} \delta_{t_s} \tag{13}$$

$$\dot{r} - \frac{I_{xz}}{I_{zz}} \dot{p} = \frac{q_v Sb}{I_{zz}} \left(C_{n_\beta} \beta + C_{n_{\delta_a}} \delta_a + C_{n_{\delta_r}} \delta_r + C_{n_{\delta_{bp}}} \delta_{bp_a} + C_{n_{\delta_{sp}}} \delta_{sp_a} \right)$$
$$+ \frac{q_{v_o} Sb^2}{2VI_{zz}} \left(C_{n_r} + C_{n_p} p \right) + N_{\delta_t} \delta_{t_a} \tag{14}$$

Total variables were defined from incremental and reference condition variables as follows:

Propulsion System Variables:

$$\left.\begin{aligned} \delta_{sp_s} &= \delta_{sp}^{\ell} + \delta_{sp}^{r} - 2\delta_{sp_o} \\ \delta_{bp_s} &= \delta_{bp}^{\ell} + \delta_{bp}^{r} - 2\delta_{bp_o} \\ \delta_{t_s} &= \delta_t^{\ell} + \delta_t^{r} \\ \delta_{i_a} &= \delta_i^{\ell} - \delta_i^{r} \end{aligned}\right\} \tag{15}$$

where i denotes a spike, bypass, or thrust variable.

Longitudinal Variables:

$$\left.\begin{aligned} \theta &= \theta_o + \Delta\theta \\ \delta_e &= \delta_{e_o} + \Delta\delta_e \end{aligned}\right\} \tag{16}$$

The horizontal and vertical forces for the reference conditions in equations (9) and (11) were calculated from the drag and lift terms by the following equations.

$$\left.\begin{aligned} X_o &= \frac{q_{V_o} S}{m}\left(C_D(0) - C_L(0)\alpha_{w_o}\right) \\ Z_o &= \frac{q_{V_o} S}{m}\left(C_L(0) + C_D(0)\alpha_{w_o}\right) \end{aligned}\right\} \tag{17}$$

Note that the transformation from stability to body axes for the lift and drag longitudinal equations was approximated differently than for the yawing and rolling moment lateral-directional equations. Since the effect of angle of attack changes were generally greater for the longitudinal equations, the lift and drag equations were continuously transformed from stability axes to body axes (eq. (9) and (11)) using the instantaneous values of angle of attack rather than only the nominal value. However, small angle approximations were used.

As indicated in previous equations, only aerodynamic nonlinearities due to angle of attack were included. These quantities were expressed in power series form as follows:

$$C^s_{D_\alpha} = C^s_{D_f} + C^s_{D_\alpha}\alpha_w + C^s_{D_{\alpha^2}}\alpha_w^2 \tag{18}$$

$$C^s_L(\alpha) = C^s_{L_f} + C^s_{L_\alpha}\alpha_w \tag{19}$$

$$C_m(\alpha) = C_{m_f} + C_{m_\alpha}\alpha_w + C_{m_{\alpha^2}}\alpha_w^2 \tag{20}$$

where the subscript f refers to the value of the quantity at $\alpha_w = 0$. Note that from the definitions used

$$\alpha_w = \alpha_{w_o} + \alpha$$

Dynamic pressure was calculated from the following approximate equation

$$q_V = \frac{1}{2}\rho(h)(V + u)^2 \tag{21}$$

For the nominal flight condition, the equation becomes

$$q_{V_o} = \frac{1}{2}\rho(h_o)V^2$$

The mass density, $\rho(h)$, was obtained from a tabulation of the 1962 atmosphere (ref. 1). The variable dynamic pressure, q_v, was replaced by the nominal value, q_{v_o}, for the smaller quantities such as damping terms in equations (9) to (14).

Incremental Mach number was calculated from the following approximate equation.

$$\Delta M = u/a_o \tag{22}$$

Small angle assumptions were used for the Euler angle transformations, flow angles, and vertical velocity equations.

$$\dot{\phi} = p \tag{23}$$

$$\dot{\theta} = q \tag{24}$$

$$\alpha = \frac{w}{V} \tag{25}$$

$$\beta = \frac{v}{V} \tag{26}$$

$$\dot{h} = V\left(\theta - \alpha_w\right) - v\phi \tag{27}$$

Definition of propulsion system coefficients— Since the simulation was concerned with interactions between the propulsion system and aircraft motions, effects of both inlet and engine exit flows on the airframe forces and moments were included. In equations (9)-(14), these effects appear as the bypass, δ_{bp}, and spike position, δ_{sp}, terms from the inlet, and the thrust, δ_t, from the engine. The following interpretation of these propulsion system terms was used. The external forces and moments on the airframe due to an element of the propulsion system can be developed from external flow changes associated with that element. The resultant forces correspond to changes in momentum and energy of the discharged flow from that present in the undisturbed flow upstream of the aircraft. Changes in the internal flow are represented in the propulsion portion of the simulation. For example, a change in bypass position has two effects. The first is a change in external forces which result from energy losses and direction changes in the flow discharged from the bypass exit. This effect appears as the bypass terms in equations (9)-(14). The second is a change in the internal inlet flow, which is calculated in the propulsion part of the simulation. This change is transmitted to the engine, and results in a second external force change due to engine thrust. Similarly, a change in spike position produces a change in the flow at the entrance to the inlet and a resulting change in external forces, as well as a change in the internal inlet flow to the engine which results in a thrust change. The external effects of the spike are relatively small in comparison with the bypass effects. While the external forces due to the bypass and spike position vary somewhat with angle of attack and Mach number, a linearized representation suitable for a restricted range of these variables was used with the simulation.

Note that when effects of inlet geometry changes on overall forces are obtained from wind tunnel results, care is needed to insure that the measurements are consistent with the definitions used for the simulation. That is, internal inlet forces need to be measured and subtracted from the overall wind tunnel values so that only external forces remain. Two additional factors must be considered in the application of wind tunnel results to the representation of flight results. The first is that the internal pressure recovery, and hence the energy of the discharged inlet flow will generally be less for the model than for the aircraft. The second is that the angle of the discharged inlet flow for the wind tunnel model may be different from that on the aircraft. Hence approximate corrections may be needed for the wind tunnel results to account for these differences in the aircraft representation.

SAS and control surface dynamics— The pitch, roll, and yaw SAS dynamics for the aircraft were represented for the high-altitude supersonic cruise conditions of interest. The system provides basic damping of the aircraft motions and utilizes primarily angular rate sensing. In addition the yaw SAS is designed to provide not only airframe damping, but also stabilization about the vertical axis during an inlet unstart. The yaw SAS uses a lateral acceleration sensor at the nose as well as a yaw rate sensor at the c.g. Effects of sensor dynamics and system gain changing with flight condition were neglected in the simulation. The equations used are as follows:

$$p_{sas} = - \frac{K_{pp} p}{1 + T_{p1} s} \tag{28}$$

$$r_{sas} = \frac{T_{r1} K_{rr} rs}{1 + T_{r1} s} + \frac{K_{rn} n_{y_n}}{1 + T_{r2} s} \tag{29}$$

where n_{y_n} is the lateral acceleration at the nose

$$q_{sas} = q \left[\frac{K_{qq}(1 + T_{q2} s)}{(1 + T_{q1} s)} + \frac{K_{q2}(1 + T_{q5} s)}{(1 + T_{q3} s)(1 + T_{q4} s)} \right] \tag{30}$$

Limits were included on the total p_{sas}, q_{sas}, and r_{sas} terms, and separately on the second order term in the q_{sas} equation.

The servo actuator dynamics for the aerodynamic control surfaces were approximated by second order equations. Provision was made in the simulation for SAS inputs, initial conditions, and external inputs. Effects of aerodynamic forces on the surfaces were neglected. The equations were expressed in the following form.

$$\text{Aileron:} \quad \frac{\ddot{\delta}_a}{\omega_{n_a}^2} + \frac{2\zeta_a}{\omega_{n_a}} \dot{\delta}_a + \delta_a = p_{sas} + p_e \tag{31}$$

$$\text{Rudder:} \quad \frac{\ddot{\delta}_r}{\omega_{n_r}^2} + \frac{2\zeta_r}{\omega_{n_r}} \dot{\delta}_r + \delta_r = r_{sas} + r_e \tag{32}$$

$$\text{Elevon:} \quad \frac{\ddot{\delta}_e}{\omega_{n_e}^2} + \frac{2\zeta_e}{\omega_{n_e}} \dot{\delta}_e + \Delta\delta_e = q_{sas} + q_e \tag{33}$$

Inlet Representation

This section describes the simulation of the inlet together with the interconnections with other portions of the system. The first part provides an overall description of the inlet and the variables used to represent it. The succeeding parts describe several portions of the simulation in more detail.

Description of inlet system— The inlet for the YF-12 aircraft is of the mixed compression type with a translating centerbody used for geometry changes. Although the inlet is basically axisymmetric, body interference effects, together with some geometry changes to adjust for these effects, result in characteristics which are somewhat unsymmetric in the presence of sideslip and angle of attack variations. Forward and aft bypass doors are provided for control of the inlet airflow. The forward door continuously modulates the flow whereas the aft door is adjusted manually to one of three positions as a function of Mach number and serves only as a coarse flow adjustment. Effects of only the forward door were included in the simulation. The inlet also has a system of bleeds on both the cowl and centerbody. Airflow from these bleeds is either dumped overboard or is ducted to the engine to provide cooling. Provision for variations in these secondary flows was not included in the simulation. Effects of inlet flow distortion and turbulence, which are of importance for inlet-engine interactions, were also neglected.

A block diagram of the inlet simulation is shown in figure 4. The representation for each inlet is the same except that the asymmetrical β functions for one side are the mirror images of the β functions for the other side. The simulation is intended to represent conditions for the started inlet up to the unstart boundary. Inlet flow dynamics for the diffuser were simplified to a first order lag term since only motions in the aircraft frequency range were of interest. Hence the principal dynamics represented were those due to control system components. The basic parameter used to represent the state of the inlet diffuser was inlet corrected airflow, w_{i_c}; i.e. diffuser airflow corrected to diffuser exit conditions. This parameter is a direct function of inlet exit geometry for the frequency range of interest. The exit changes result from variations in the forward bypass opening and from changes in the airflow demanded by the engine.

Three other inlet parameters were determined - (1) pressure recovery, (2) bypass signal pressure ratio, and (3) terminal shockwave position. Inlet pressure recovery is a parameter affecting engine performance and is a primary input to the engine. The bypass signal pressure ratio is needed for the representation of the bypass control system and terminal shock-wave position represents the margin of the inlet from the unstart condition. A major problem in the simulation was the incorporation of wind tunnel results to provide an adequate representation of these three quantities. Wind tunnel data included in a Lockheed Aircraft Corp. report of a detailed digital computer simulation of the inlet indicated that the quantities are nonlinear functions of five variables. The two variables which have primary effects are the inlet variables: corrected inlet airflow and spike position. Three more variables, which have a secondary effect, are those describing entrance conditions to the inlet: angle of attack, sideslip angle, and Mach number. A complete tabular representation of functions of this many variables, even over restricted ranges, would result in a rather cumbersome and slow computational procedure. A simpler approach for the purpose of generating time histories was to first curve-fit the multi-dimensional wind tunnel data by a power series expansion in several variables. Each function was then determined from the series as needed during the computation of the time history.

Inlet pressure representation— The coefficients of the series representing the pressure recovery and bypass signal pressure functions were obtained through use of a least square criterion. Care was necessary in selecting the range to be curve fitted and the resulting number of coefficients to be used in order to keep the representations as simple as possible. As previously mentioned, these pressures were represented as functions of two primary variables, the inlet variables, w_{i_c}, and δ_{sp}, and three secondary variables, α, β, and M. The functional representation was expressed as follows. For a nominal condition of the three secondary variables, an expansion was made of the two primary inlet variables, w_{i_c}, and δ_{sp}. Expansions of the primary variables were also made with each of the secondary variables. Note that this procedure neglects terms containing crossproducts between the secondary variables. In these expressions, the expansions for the inlet variables, w_{i_c} and δ_{sp}, were made relative to convenient average inlet conditions, while the expansions for the secondary variables were made relative to the particular nominal flight condition. The former choice was made in order to facilitate adjustment of the inlet operating condition. Hence, for a set of nominal values of α and M ($\beta = 0$), the pressure recovery and bypass signal pressures were determined by the following expressions (fig. 4):

$$\frac{p_{t_2}}{p_{t_o}} = f_a\left(w_{i_c}, \delta_{sp}\right) + f_a\left(w_{i_c}, \delta_{sp}, \alpha\right) + f_a\left(w_{i_c}, \delta_{sp}, \beta\right) + f_a\left(w_{i_c}, M\right) \tag{34}$$

$$\frac{p_s}{p_{t_m}} = f_b\left(w_{i_c}, \delta_{sp}\right) + f_b\left(w_{i_c}, \delta_{sp}, \alpha\right) + f_b\left(w_{i_c}, \delta_{sp}, \beta\right) + f_b\left(w_{i_c}, M\right) \tag{35}$$

The series expansions for each of the f functions were expressed as

$$f\left(w_{i_c}, \delta_{sp}, X\right) = \sum_{i=0}^{i_{max}} \sum_{j=0}^{j_{max}} \sum_{k=1}^{k_{max}} C_{ijk} w_{i_c}^{i} \delta_{sp}^{j} X^{k} \tag{36}$$

where the quantity, X, represents α, β, or M. The upper limits used, which determine the number of coefficients required for each pressure function, are listed in Table 1. In the selection of the coefficients, C_{ijk}, an attempt was made to provide a balance between accuracy required and the need to maintain computational time as short as possible. Interpolation of the functions was also necessary in order to obtain expansions about the desired nominal flight conditions. The procedures used for determining these coefficients are described in Appendix A.

As previously stated the input variables were expanded relative to convenient average inlet conditions. Hence, for a particular reference condition, steady state corrections were necessary to set the nonlinear functions at the correct values and to interface with linear portions of the simulation. The corrections provided a means for adjusting the inlet to different reference conditions. The quantities, δ_{sp_o} and w_{ic_o} (fig. 4), were used to define the inlet nominal operating conditions and, hence, to calculate nominal values of the nonlinear pressure and unstart functions. The quantity, $\left(p_s/p_{t_m}\right)_o$, was calculated to null the signal error for the inlet nominal conditions so that a proper interface with the incremental bypass position, $\Delta\delta_{bp}$, would be obtained. The quantity, $\left(p_{t_2}/p_{t_o}\right)_o$ was calculated to null the pressure recovery signal to the linearized engine for nominal conditions. Note that these corrections are distinct from initial condition selections.

Shockwave position and unstart boundaries— An additional calculation was made to obtain the inlet unstart boundaries and shockwave position as a function of distance from the unstart condition. The calculation was based on a power series expansion of wind tunnel results (contained in a Lockheed Aircraft Corp. report) with respect to a nominal flight condition. The form for the inlet unstart boundary to be represented as a function of inlet parameters (with fixed α, β and M) is shown in sketch a. The lower boundary in the sketch represents the effect of restricting the inlet exit flow so that unstart occurs and will be called the airflow boundary. The left hand boundary represents the effect of overcontracting the area ratio at the inlet entrance with the spike so that unstart occurs, and will be called the spike boundary. These

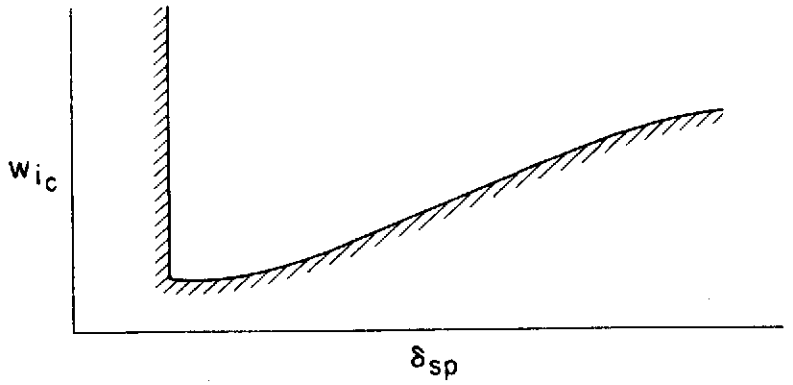

Sketch (a)

boundaries are affected primarily by changes in M and also by variations in α and β. The data for the unstart boundaries were obtained from steady-state wind tunnel tests. Because of the relatively low frequency of the disturbing quantities relative to the basic inlet dynamics, dynamic effects on unstart were not considered significant.

An examination of available wind tunnel data resulted in the following functional forms for the unstart boundaries. The relation of each function to the rest of the inlet simulation is indicated in figure 4. In curve fitting the data, effects of α, β, and M were represented separately since effects of simultaneous variations in these quantities were felt to be of higher order. The basic airflow and spike boundaries, with M corrections added, were expressed as follows:

Airflow Boundary, $f_{c_a}\left(\delta_{sp_d}\right)$, $f_{c_a}\left(\delta_{sp}, M\right)$:

$$\left.\begin{aligned} &\text{For } \delta_{sp_1} \leqslant \delta_{sp_d} \leqslant \delta_{sp_2} \\ &\qquad f_{c_a}\left(\delta_{sp_d}\right) = w_{i_2} \\ &\text{For } \delta_{sp_d} \geqslant \delta_{sp_2} \\ &\qquad f_{c_a}\left(\delta_{sp_d}\right) = w_{i_2} + K_{c_1}\left(\delta_{sp_d} - \delta_{sp_2}\right) \end{aligned}\right\} \tag{37}$$

where $\delta_{sp_d} = \delta_{sp} + K_{i_{12}} \Delta M$

$$f_{c_a}\left(\delta_{sp}, M\right) = -K_{i_{15}} \Delta M + K_{i_{16}} \delta_{sp} \Delta M \tag{38}$$

Spike boundary, $f_{c_s}\left(\delta_{sp_d}\right)$:

$$f_{c_s}\left(\delta_{sp_d}\right) = \delta_{sp_d} - \delta_{sp_3} \tag{39}$$

All of the quantities in equations (37) and (39) with numbered subscripts denote constants. The M corrections provide both slope and displacement changes to the airflow unstart boundary.

Separate α and β functions were applied to obtain displacement corrections for the airflow and spike unstart boundaries. These functions were of the following form:

Angle of attack correction:

$$\left.\begin{aligned} f_{c_a}(\alpha) &= K_{i26}\alpha + K_{i27}\alpha^2 \\ f_{c_s}(\alpha) &= K_{i28}\alpha + K_{i29}\alpha^2 \end{aligned}\right\} \tag{40}$$

Sideslip angle corrections:

For $\beta \leqslant 0$,

For $\beta \geqslant 0$,

$$\left.\begin{aligned} f_{c_a}(\beta) &= K_{i21}\beta^2; \quad f_{c_s}(\beta) = K_{i24}\beta^2 \\ f_{c_a}(\beta) &= K_{i22}\beta^2; \quad f_{c_s}(\beta) = K_{i25}\beta^2 \end{aligned}\right\} \tag{41}$$

As indicated in figure 4, the unstart airflow boundary, $w_{i_{c_u}}$, is the sum of the airflow boundary nonlinear functions.

$$w_{i_{c_u}} = f_{c_a}\left(\delta_{sp_d}\right) + f_{c_a}\left(\delta_{sp}, M\right) + f_{c_a}(\alpha) + f_{c_a}(\beta) \tag{42}$$

Similarly, the unstart spike boundary is the sum of the spike boundary functions.

$$\delta_{sp_u} = f_{c_s}\left(\delta_{sp_d}\right) + f_{c_s}(\alpha) + f_{c_s}(\beta) \tag{43}$$

The shockwave position was curve-fitted from wind tunnel data as a nonlinear function, $f_d(w_{i_c})$, of incremental airflow from the unstart boundary.

$$x_s = K_{i32}\Delta w_c + K_{i33} \sin\left(K_{i34}\Delta w_c\right) \tag{44}$$

where

$$\Delta w_c = w_{i_c} - w_{i_{c_u}}$$

The function was assumed to be independent of inlet and flight conditions for the operating range of interest. An inlet unstart, which could result from either the airflow or spike boundaries being exceeded, was indicated by either of the following equations:

$$x_s \leqslant 0, \quad \text{or} \quad \delta_{sp} \leqslant \delta_{sp_u} \tag{45}$$

The simulation was terminated when an unstart occurred since unstart conditions were not represented.

Inlet control system— The inlet control system positions the spike as a function of flight condition, and bypass flow as a function of flight condition and engine airflow demand. The objective is to maintain the inlet airflow at as high a performance condition, i.e. high pressure recovery and minimum flow distortion, as possible while still preventing an inlet unstart. The spike position is determined by an open loop command function which is computed from flight condition measurements. Bypass flow is adjusted by closed loop control with the forward bypass doors. The bypass signal is a pressure signal indicative of the position of the terminal shockwave in the inlet. It is formed from a combination of several static pressure sources which are summed and divided by a signal which is an approximate measurement of free stream total pressure. The use of this latter measurement reduces effects of dynamic pressure changes on the control signal. The signal is represented by a single variable, p_s/p_{t_m}, in the simulation. The desired pressure signal is a function of flight condition measurements.

The inlet control command signals and bypass loop are included in figure 4. The flight condition measurements, α, β, M, and n_z were used as open loop commands to both the spike and bypass controls. Dynamics associated with these measurements were represented by the time constants, T_α, T_β, and T_M. The effect of α, β, M, and n_z command signals to the spike were represented by the functions $f_{sp}(\alpha_m)$, K_{i12}, $f(\beta)$, K_{i19}, and $f_{sp}(n_z)$ respectively. Similarly command signal corrections used for the bypass pressure ratio setpoint were $f_{bp}(\alpha M)$, K_{i10}, $f(\beta)$, and $f_{bp}(n_z)$. The command functions were expressed as power series expansions as follows:

Spike commands:

$$\Delta f_{sp}\left(\alpha_{w_m}\right) = f_{sp}\left(\alpha_{w_m}\right) - f_{sp}\left(\alpha_{w_o}\right) \tag{46}$$

where

$$f_{sp}\left(\alpha_{w_m}\right) = \sum_{i=2}^{3} a_{s\alpha i} \left|\alpha_{w_m} - 5.0\right|^i$$

$$\alpha_{w_m} = \alpha_{w_o} + \alpha_m$$

$$f_{sp}\left(M_m\right) = K_{i19}\Delta M_m \tag{47}$$

$f_{sp}\left(n_{z_m}\right)$:

$$\left.\begin{aligned}
&\text{For } |n_{z_m}| \geq \ell_1, \\
&\qquad f_{sp}\left(n_{z_m}\right) = a_{sn_z}\left(|n_{z_m}| - \ell_1\right) \\
&\text{For } |n_{z_m}| \leq \ell_1, \\
&\qquad f_{sp}\left(n_{z_m}\right) = 0
\end{aligned}\right\} \tag{48}$$

where ℓ_1 is a constant.

Bypass commands:

$$\Delta f_{bp}\left(\alpha_{w_m}, M_m\right) = f_{bp}\left(\alpha_{w_m}, M_m\right) - f_{bp}\left(\alpha_{w_o}, 0\right) \tag{49}$$

where

$$f_{bp}\left(\alpha_{w_m}, M_m\right) = \sum_{i=0}^{3}\sum_{j=1}^{2} a_{ij}\alpha_{w_m}^{i}\Delta M_m^{j}$$

$f_{bp}\left(n_{z_m}\right)$:

$$\left.\begin{aligned}
&\text{For } |n_{z_m}| \geq \ell_1, \\
&\qquad f_{bp}\left(n_{z_m}\right) = a_{bn_z}\left(|n_{z_m}| - \ell_1\right) \\
&\text{For } |n_{z_m}| \leq \ell_1, \\
&\qquad f_{bp}\left(n_{z_m}\right) = 0
\end{aligned}\right\} \tag{50}$$

Spike and bypass command:

$f(\beta_m)$:

For $\beta_m \leq 0$,

$$f(\beta_m) = \sum_{i=2}^{3} a_{\beta i} \beta_m^i$$

For $\beta_m \geq 0$,

$$f(\beta_m) = \sum_{i=2}^{3} b_{\beta i} \beta_m^i \qquad (51)$$

Note that the command functions are expressed as incremental values from nominal conditions.

The bypass control loop consisted of the bypass control dynamics and the previously described diffuser dynamics and signal pressure function (fig. 4). The bypass actuator dynamics and filtering were simplified to the second order form shown. Effects of M changes on the bypass control gain were neglected.

Engine Representation

The simulation represented the dynamic response of the engine operating in the afterburning mode and a block diagram is shown in figure 5. The simulation for each engine was identical. The response was linearized relative to a selected nominal condition. Hence, all engine states shown in figure 5 are incremental values from the nominal condition and the Δ symbol denoting increments has been omitted. The primary purpose of the engine representation was to provide input-output relationships for those variables which directly interacted with other portions of the aircraft systems. However, sufficient depth of the representation was considered necessary to also provide a basis for comparisons with subsequent flight-test results. The principal relationships represented consisted of the dynamic response of engine thrust, compressor airflow, and fuel flows to throttle position and inlet pressure recovery. Response to the latter input was included since it represented the principal interconnecting parameter from the inlet to the engine. The compressor corrected airflow, w_{e_c}, response was needed since this quantity was the the principal interconnecting parameter from the engine to the inlet.

Effects of variations in flight condition, i.e. Mach number, M, and dynamic pressure, q_v, on the engine response were also represented. These quantities were input to the engine simulation at the pressure disturbance location with the gain functions, K_{i23} and $f_1(M)$ based on calculated thrust changes. The gains were determined from steady-state variations in calculated thrust due to each input parameter with the other parameter held constant. The quantity, q_v, produces an engine dynamic response which is similar to a

p_{t_2}/p_{t_o} input since a compressor inlet pressure change occurs in both cases. Hence, these two inputs were added at the same point for the simulation. However, the M disturbance produces engine dynamic responses somewhat different from p_{t_2}/p_{t_o} since it introduces compressor inlet temperature changes. Since the frequency content of the M disturbance is relatively low in comparison with the engine dynamics, the representation of the difference in the dynamic response due to this disturbance from a p_{t_2}/p_{t_o} disturbance was not considered necessary. Hence, the M disturbance was introduced in the same manner as the pressure disturbances. As previously mentioned, the gains from the q_v and M inputs were determined from the variations in steady-state thrust only. Hence, although qualitatively the same, the resulting changes in fuel-flow and burner pressure due to M inputs were somewhat in error. Note, however, that these engine variables are of less importance than others since they are not fed back to other portions of the simulation.

Corrections due to M inputs were also applied to the engine compressor airflow variable by means of the gain K_{i20}. The gain was estimated through use of a linearization of steady-state compressor operating curves and the corrected airflow relationship. An additional consideration was that a change in compressor inlet temperature due to M would result in a slight change in trimmed rotor speed. This effect was neglected in the rotor speed calculation but was included in the selection of the gain for the engine airflow calculation.

Once the form of the engine simulation was established, numerical values of the dynamic coefficients were obtained by matching time histories computed from this simulation with results computed from a more extensive simulation of the engine which included nonlinear representations of all major engine components. The engine simulation is described in a report by the Pratt & Whitney Div. of United Aircraft Corp. For a desired nominal operating condition, responses of installed thrust, fuel flow, burner pressure, and rotor speed to throttle and pressure recovery inputs were used for the comparison.

Numerical Integration Techniques

The methods used for numerical integration of the dynamic equations previously described are given in this section. In selecting the integration method to be used for achieving a certain accuracy level, careful attention must be given to tradeoffs in computational time, levels of complexity in the method itself, and the maximum allowable size of the integration step. This tradeoff will also depend on the degree of complexity of the system representation including the nonlinear relationships present.

Two basic integration methods, which were intended for use with fixed step size integration, were applied to different portions of the simulation. The first was an equation of motion method for integration of a set of first order differential equations. This method was used to integrate the aircraft equations of motion. The second method involved the determination of the

response of linear portions of the system to a step input during each integration interval and is called the z-transform method. This method was used for the remaining portions of the system - SAS, inlet, engine, and their controls.

For the equation of motion method, the following second order Adams-Bashford predictor equation (e.g. ref. 2) was used to obtain the value of the vector state Y at time t_{k+1} from known values at times t_k and t_{k-1}.

$$Y\left(t_{k+1}\right) = Y\left(t_k\right) + \left[3Y'\left(t_k\right) - Y'\left(t_{k-1}\right)\right] (T/2) \tag{52}$$

where the continuous 1st order differential equation is given by the vector form

$$Y' = f(t,Y)$$

The method involved prediction by means of a polynomial curve fit of present and past values of each state variable to be integrated. While a higher order integration algorithm involving more past terms in Y' could have been used, some computational experimentation indicated that an overall improvement would not be obtained. In order to maintain a certain accuracy level, the computation interval could not be increased sufficiently to compensate for the additional time required to compute the higher order form. A basic problem in using this integration method occurs when a large dynamic range of equations is present. If the step size selected is too large for the higher frequency dynamics, the calculation can go unstable since the derivative for the high frequency equation is assumed constant for too large an increment of time.

One method for improving computational accuracy for the higher frequency portions of the system is to integrate those equations in closed form with the assumption of a known input over the integration interval. The z-transform method can be used to find the output of a linear dynamic element to a selected input over a sampling interval, T. This approach is particularly useful for a system represented in block diagram form. An example of the application of the z-transform method to numerical integration is included in reference 3. Note that the method can still be used for a nonlinear system as long as the system can be separated into zero memory nonlinearities and linear dynamics. The simplest form of input to use is a step that is assumed constant over the integration interval. However, the input actually changes during the interval. If the value of the input at the beginning of the interval is used for the entire interval, a time delay is introduced which can result in an unstable calculation for a system with feedback loops. One way to include the effect of the changing input, with values known at the beginning and end of the interval, would be to determine the response of the linear element to a ramp input. A simpler approach, which was actually used, is to employ the equations for the step response but to average the input over the sampling interval.

This averaging was done as follows. For locations where the input was known at both the beginning and end of the sampling interval, the average value of the input was directly calculated by the following equation.

$$r_{av} = \frac{1}{2}\left[r\left(t_k\right) + r\left(t_{k+1}\right)\right] \tag{53}$$

This computation was possible for instance when integrating a state with an input which was previously integrated through use of the equations of motion method. However, the value of the input at the end of the sampling interval may not always be available. For instance at feedback junctions, the updated value of the returned quantity generally is not known. A typical situation is shown in sketch (b).

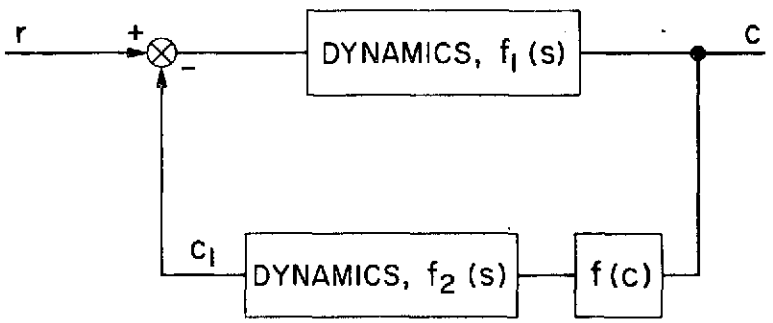

Sketch (b)

The input, r, was assumed known up to and including the time, t_{k+1}. States in the feedback loop dynamics including the output, c, were known only up to the time t_k. In order to average both inputs to $f_1(s)$, an estimate of c_1 for the interval t_k to t_{k+1} was needed. The following predicted average equation was used for this situation.

$$c_{1_{av_p}} = \frac{1}{2}\left[3c_1\left(t_k\right) - c_1\left(t_{k-1}\right)\right] \tag{54}$$

Again it was felt that the use of a higher order prediction equation would not allow a sufficient increase in sampling time to compensate for the resulting increased computational time. The predicted coefficient, $c_{1_{av_p}}$ was then combined with a time averaged r coefficient to form an averaged error input to $f_1(s)$. The integration algorithm was then applied to obtain $c\left(t_{k+1}\right)$. Next the outputs of the remaining quantities in the loop, f(c) and $f_2(s)$ were computed for the time t_{k+1}. While the procedure could have been iterated further through use of the quantity, $c_1\left(t_{k+1}\right)$, it was not considered necessary. Similar procedures using input averaging and prediction, where necessary, can be applied to more general feedback structures, and also to systems of first order equations.

For the YF12 simulation, the airframe motion dynamics were expressed in first order form and integrated by means of the equations of motion method (eq. 52). All other components, the SAS, inlet, and engine, and their controls, were integrated by the z-transform method with the components in block diagram form. A subprogram was used to compute z-transform coefficients which represented responses of first or second order transfer functions to a step input. Input averaging (eq. (53) and (54)) was included for cases in which the frequency content of the input was sufficiently high to result in some variation during the integration interval. The simulation operated in real time with a step size of 0.02 seconds.

CONCLUDING REMARKS

The simulation was intended for use both for the identification of parameters by comparison with flight test results, and for control system studies. Only preliminary flight measurements of SAS-off Dutch-roll oscillations have been available and these measurements allow a comparison with only a portion of the simulation. The flight measurements indicated a reduction in Dutch-roll damping due to activity of the inlet control system and results from the simulation indicated similar changes. Hence, on the basis of available flight data, the simulation is felt to exhibit adequate sensitivity to parameter variations.

APPENDIX A

REGRESSION ANALYSIS FOR NONLINEAR PRESSURE FUNCTIONS

The requirements for determining the coefficients for the polynomial expansion for the inlet nonlinear pressure functions are outlined in this section. The effort involves selecting the form of the expansion and obtaining a least squares fit of the data for the range of interest. To date these computations were performed separately although a general program could be prepared to compute all necessary coefficients in sequence and output them in a punched card form suitable for use in the 8400 digital computer program. The necessary mathematical steps are outlined in the following paragraphs.

The polynomial expansions of the pressure variables were obtained from wind tunnel data which are functions of five independent variables. Two variables were considered to be primary ones, w_{i_c}, δ_{sp}, to be fitted with greater accuracy, and the remaining variables, α_w, β, M, were considered secondary and were fitted less accurately. Polynomials of prescribed form were fitted to the data using a least square criterion. A factor to be accounted for in the curve-fitting process was that the range for which the inlet variables $\left(w_{i_c}, \delta_{sp}\right)$ were needed varied with flight condition. A double interpolation of a portion of the polynomial coefficients was also required since, in general, the expansions were made relative to nominal conditions which were different from the original data conditions.

The complete polynomial expansion for either the pressure recovery or signal pressure function, P, was expressed in the following form by the substitution of equation (36) into equation (34) or (35)

$$\left.\begin{aligned} P\left(\alpha_{w_o}, 0, M_o\right) = & \sum_{i=0}^{i_{max}} \sum_{j=0}^{j_{max}} C_{ij} w_{i_c}^{i} \delta_{sp}^{j} \\ & + \sum_{i=0}^{i_{max_k}} \sum_{j=0}^{j_{max}} \sum_{k=1}^{k_{max}} C_{ijk} w_{i_c}^{i} \delta_{sp}^{j} \alpha^{k} \\ & + \sum_{i=0}^{i_{max_\ell}} \sum_{j=0}^{j_{max}} \sum_{\ell=1}^{\ell_{max}} C_{ijk} w_{i_c}^{i} \delta_{sp}^{j} \beta^{\ell} \\ & + \sum_{i=0}^{l} C_{im} w_{i_c}^{i} \Delta M \end{aligned}\right\} \qquad \text{(A1)}$$

Note that the expansion is made relative to nominal flight condition of $\alpha_w = \alpha_{w_o}$, $\beta = 0$, and $M = M_o$. Also, the incremental angle of attack is defined as $\alpha = \alpha_w - \alpha_{w_o}$. As previously discussed, provision was made to expand the inlet variables, w_{i_c} and δ_{sp}, about any convenient average inlet condition. The upper summation limits for each pressure function are given in Table 1. The procedure for obtaining the coefficients was separated into the following steps.

The first step was to perform a linear regression for the two primary variables, w_{i_c} and δ_{sp}, for values of α_w, β, M for which wind tunnel data were available. Hence, the form of the first summation in equation (A1), denoted by P_1, was used to determine the regression equation for the unknown coefficients $C_{ij}(\alpha_w, \beta, M)$.

$$P_1(\alpha_w, \beta, M, J) = \sum_{i=0} \sum_{j=0} C_{ij}(\alpha_w, \beta, M) w_{i_c}^i(J) \delta_{sp}^j(J) \qquad \text{(A2)}$$

where

$$J = 1 \cdots N(\alpha_w, \beta, M)$$

The value, $N(\alpha_w, \beta, M)$, is the number of data points used to determine $P_1(\alpha_w, \beta, M)$ as a function of w_{i_c} and δ_{sp} for each constant (α_w, β, M) condition.

The second step was to interpolate the C_{ij} coefficients in the α and M directions to selected nominal values of α_{w_o} and M_o. Both linear (using two values per direction) and quadratic (using three values per direction) interpolations were used. The choice depended upon the variations in the coefficients between data points in the α_w and M directions. An available single direction interpolation program was successively applied as follows.

$$C_{ij}(\alpha_w, \beta, M) \xrightarrow{M} C_{ij}(\alpha_w, \beta, M_o)$$

$$C_{ij}(\alpha_w, \beta, M) \xrightarrow{\alpha} C_{ij}(\alpha_{w_o}, \beta, M)$$

$$C_{ij}(\alpha_{w_o}, \beta, M) \xrightarrow{M} C_{ij}(\alpha_{w_o}, \beta, M_o)$$

where the subscript o refers to the selected nominal value of the M or α_w variable.

The third step was to perform a linear regression for the primary variables with each of the secondary variables, α, β, M, as indicated by the second, third, and fourth summations in equation (A1). The resulting expansions were made relative to the nominal conditions selected in the previous interpolation. For instance, for the α variable, the regression equations for the unknown C_{ijk} coefficients were as follows:

$$P_2\left(\alpha,\ 0,\ M_o,\ J\right) = \sum_{i=0}^{i_{max}} \sum_{j=0}^{j_{max}} \sum_{k=1}^{2} C_{ijk}\left(\alpha_{w_o},\ 0,\ M_o\right) w_{i_c}^{i}(J)\,\delta_{sp}^{j}(J)\,\alpha^{k}(J) \qquad \text{(A3)}$$

where

$$J = 1 \cdot \cdot \cdot N\left(0,\ M_o\right)$$

The quantity, $N\left(0,\ M_o\right)$, is the number of data points used to determine $P_2\left(\alpha,\ 0,\ M_o\right)$ as a function of w_{i_c}, δ_{sp}, and α.

The function, $P_2\left(\alpha,\ 0,\ M_o,\ J\right)$ was computed from the following equation.

$$P_2\left(\alpha,\ 0,\ M_o,\ J\right) = P_1\left(\alpha_w,\ 0,\ M_o,\ J\right) - P_1\left(\alpha_{w_o},\ 0,\ M_o,\ J\right) \qquad \text{(A4)}$$

The functions, $P_1\left(\alpha_w,\ 0,\ M_o,\ J\right)$ and $P_1\left(\alpha_{w_o},\ 0,\ M_o,\ J\right)$, were determined through use of the first summation given in equation (A1) and the appropriate C_{ij} coefficients. For instance, the equation for $P_1\left(\alpha_{w_o},\ 0,\ M_o,\ J\right)$ is

$$P_1\left(\alpha_{w_o},\ 0,\ M_o,\ J\right) = \sum_{i=0}^{i_{max}} \sum_{j=0}^{j_{max}} C_{ij}\left(\alpha_{w_o},\ 0,\ M_o\right) w_{i_c}^{i}(J)\,\delta_{sp}^{j}(J) \qquad \text{(A5)}$$

A similar procedure was used to obtain the expansions for the β and M variables in equation (A1).

APPENDIX B

SIMULATION PROGRAM LISTING

A listing of the computer program for the representation of the YF12 aircraft motions and propulsion system dynamics is provided in this section. A list of the principal fortran variables is given in Table 2. Listings of other subroutines used in the execution of the simulation such as an executive monitoring program, which provides overall control, and numerical integration programs are not included.

The subprograms shown in the listing are used in the following sequence. In subroutine SETUP, the necessary initial quantities are calculated for use in subsequent portions of the simulation. Each integration step is controlled by subroutine LOOP1. This subroutine calls, in turn, the subroutines for the various parts of the simulation - INLET, ENGINE, CONTRL (SAS), and AIRFRM. In each of these subroutines, the necessary constants for the dynamic equations are calculated and calls are made to the appropriate integration subroutines when needed. Brief descriptions of several additional subroutines which are called in the listing are as follows.

ZXFORM - This subroutine calculates the coefficients to be used in the z-transform integration as a function of transfer function coefficients and integration interval.

XFERDA - This subroutine is used in scaling, biasing, and time multiplexing signals to be output to analog recorders.

MGRATE - This subroutine is the initialization portion of the equation of motion integration method. The number of variables to be integrated, order of integration, and step size are established.

GRATON - This subroutine computes and stores results for an integration interval for the equations-of-motion integration method.

ARDC62 - This subroutine is a tabulation of density and speed of sound versus altitude for the 1962 ARDC atmosphere.

VALLMT - This function supplies limits for an indicated variable.

The computer listing for the aircraft equations is as follows.

```
C       TITLE                                   SETUP
        SUBROUTINE SETUP
C
        COMMON /BLK1 / IMODE    ,IDT      ,ITIMES   ,DT       ,NDT
       1,     TIME     ,D2R      ,ID
C
        COMMON /BLK2 / UB       ,VB       ,WB       ,PB       ,QB
       1,     PB       ,PHIR     ,THETR    ,PSIR     ,PHI      ,THET
       2,     PSI      ,DM       ,BETA     ,ALFA     ,BETAR    ,ALFAR
       3,     ALT      ,ANY      ,ANZ      ,CLB      ,CLBA     ,CLDR
       4,     CLDBR    ,CLDSR    ,CLRB     ,CLPB     ,CNB      ,CNDA
       5,     CNDR     ,CNDBR    ,CNRSR    ,CNRB     ,CNPB     ,DELTAA
       6,     DELTAE   ,DELTAR   ,G2Z      ,S2Z      ,PS2      ,PT2Z
       7,     DSP(2)   ,DBP(2)   ,PT2S(2)  ,PLA(2)   ,AJC(2)   ,RPMM(2)
       8,     T(2)     ,WEC1(2)  ,DQBAR
C
        COMMON /BLK3 / CDZ      ,CDA1     ,CDA2     ,CL7      ,CLA1
       1,     CMZ      ,CMA1     ,CMA2     ,CDDE     ,CDDBR    ,CDDSR
       2,     CLFDE    ,CLFDBR   ,CLFDSR   ,CLFCB    ,CBARZ    ,VZ
       3,     AREA     ,XMASS    ,CHORD    ,SPAN     ,G        ,XXT
       4,     XZT      ,XLT      ,XMT      ,XNT      ,XIXX     ,XIYY
       5,     XIZZ     ,XIXZ     ,CYB      ,CYDR     ,CYPR     ,CLAR
       6,     CMA0     ,CMQB     ,CMDE     ,CMDBR    ,CLRS     ,CLPBS
       7,     CLRBS    ,CLDAS    ,CLDRS    ,CLDBRS   ,CLPSRS   ,CNRS
       8,     CNPBS    ,CNRBS    ,CNDAS    ,CNDRS    ,CNPBRS   ,CNDSRS
C
        COMMON /BLK5 / XKPP     ,XKQQ     ,XKQ2     ,XKPR     ,XKRN
       1,     TC1      ,TC2      ,TCN1     ,TCD1     ,TCN2     ,TCD21
       2,     TCD22    ,TCN3     ,WNA      ,ZA       ,WNF      ,ZE
       3,     WNR      ,ZR       ,T11      ,T12      ,T14      ,WNSP
       4,     ZSP      ,TE1      ,TE2      ,TE4      ,TED1     ,TEN2
       5,     TED2     ,TIDA     ,TIDB     ,TIDM
C
        COMMON / BLK7 / G1A     ,G1B      ,G1C      ,G1D      ,G2A
       1,     G2B      ,G2C      ,G2E      ,G2F      ,G3C      ,G2H
       2,     G2I      ,G2J      ,G2K      ,G2L      ,G3A      ,G3B
       3,     G4A      ,G4B      ,G4C      ,G4D      ,G4E      ,G4F
       4,     G5A      ,G5B      ,G5C      ,G6A      ,G7A      ,G7B
       5,     G7C      ,G7D      ,G9A      ,G8F      ,G8C      ,G8D
       6,     G9E      ,G8F      ,G8G      ,G8H      ,G8I      ,G8J
       7,     G6K      ,G6L
C
        COMMON /BLK8 / G9A      ,G9B      ,G9C      ,G9D      ,G9E
       1,     G9F      ,G10A     ,G11A     ,G11B     ,G11C     ,G11D
       2,     G11E     ,G11F     ,G11G     ,G12A     ,G12B     ,G14A
       3,     G14B     ,G14C     ,G14D     ,G14E     ,G14F     ,G15A
       4,     G15B     ,G15C     ,G15D     ,G16A     ,G16B     ,G16C
       5,     G16D     ,G16E     ,G16F     ,G16G     ,G16H     ,G17A
       6,     G17B     ,G17C     ,G19A     ,G18B     ,G18C
       7,     G19A     ,G19B     ,G20A     ,G20B
C
        COMMON /BLK10/ GN1(17)  ,FR1(17)  ,Z01(17)  ,Z11(17)  ,GN2(4)
       1,     A2ND(4)  ,B2ND(4)  ,Z021(4)  ,Z022(4)  ,Z121(4)  ,Z122(4)
C
        COMMON /BLK11/ ALFAZ    ,ALFAZR   ,DSPZ     ,WICZ     ,DBPZ
       1,     THETZ    ,DEZ      ,PBIC     ,QBIC     ,RBIC     ,PHIIC
       2,     THEIC    ,PSIIC    ,DMIC     ,BETAIC   ,ALFAIC   ,ALTIC
       3,     ICDSP(2) ,DSPIC(2) ,DSPDIC(2),ICDBP(2) ,DBPIC(2) ,DBPDIC(2)
       4,     ICRPM(2) ,RPMIC(2) ,ICAJ(2)  ,AJIC(2)  ,AJDIC(2) ,AJCDIC(2)
       5,     ICWFAB(2),WFABIC(2),ICWFPB(2),WFPBIC(2),ICPSAS   ,PSASIC
       6,     PSADIC   ,ICQSAS   ,QSASIC   ,ICRSAS   ,PSASIC   ,RSASDIC
       7,     RSAIIC   ,RSA2IC   ,ICDA     ,DAIC     ,DADIC    ,ICDE
       8,     DEIC     ,DEDIC    ,ICDR     ,DRIC     ,DRDIC    ,X9
       9,     ZB       ,XMP      ,ALTZ
C
C
        DIMENSION IORD(4)
C
        DATA NUM1/17/,NUM2/4/,IORD/4*0/
C
        ID=1
C
        DT=.001*IDT
C
C  INITIALIZE
C
        TIME=0.0
```

```
C
      PB=PBIC*D2R
      QB=QBIC*D2R
      RB=RBIC*D2R
C
      PHI  =PHIIC
      PHIR =PHI*D2R
      THET =THEIC
      THETR=THET*D2R
      PSI  =PSIIC
      PSIR =PSI*D2R
C
      DH    =DMIC
      BETA  =BETAIC
      BETAR =BETA*D2R
      ALFA  =ALFAIC
      ALFAR =ALFA*D2R
      ALFAZR=ALFAZ*D2R
C
      UB=DH*968.
      VB=BETAP*VZ
      WB=ALFAP*VZ
C
      ALT=ALTIC
C
C  QUANTITIES RELATED TO REFERENCE CONDITIONS
C
      PSZ =-(G9A+G9B*DSPZ+(G9C+G9D*DSPZ+(G9E+G9F*DSPZ)*WICZ)*WICZ)
C
      PT2Z=-(G15A+G15B*DSPZ+(G15C+G15D*DSPZ)*WICZ)
C
      DSU1=ALFAZ*ALFAZ
      DSU2=ALFAZ*DSU1
      G2Z =G2A*DSU2+G2B*DSU1+G2C*ALFAZ
C
      DSU3=ABS(ALFAZ-G7A)
      DSU4=DSU3*DSU3
      DSU5=DSU3*DSU4
      G7Z =G7B*DSU5+G7C*DSU4+G7D*DSU3
C
C  STABILITY DERIVATIVES CONVERTED FROM STABILITY AXES TO BODY AXES
C
      CALFAZ=COS(ALFAZR)
      SALFAZ=SIN(ALFAZR)
      CALFZ2=CALFAZ*CALFAZ
      SALFZ2=SALFAZ*SALFAZ
      DSU6  =(CNPBS+CLRBS)*SALFAZ*CALFAZ
      DSU7  =(CLPBS-CNRBS)*SALFAZ*CALFAZ
C
      CNB   =CNBS*CALFAZ+CLBS*SALFAZ
      CLB   =CLBS*CALFAZ-CNBS*SALFAZ
      CNRB  =CLPBS*SALFZ2+CNRBS*CALFZ2+DSU6
      CLPB  =-CNPBS*SALFZ2+CLRBS*CALFZ2+DSU7
      CNPB  =-CLRBS*SALFZ2+CNPBS*CALFZ2+DSU7
      CLPB  =CNRBS*SALFZ2+CLPBS*CALFZ2-DSU6
      CNDR  =CNDRS*CALFAZ+CLDRS*SALFAZ
      CLDR  =CLDRS*CALFAZ-CNDRS*SALFAZ
      CNDA  =CNDAS*CALFAZ+CLDAS*SALFAZ
      CLDA  =CLDAS*CALFAZ-CNDAS*SALFAZ
      CNDBP =CNDBPS*CALFAZ+CLDBPS*SALFAZ
      CLDBP =CLDBPS*CALFAZ-CNDBPS*SALFAZ
      CNDSP =CNDSPS*CALFAZ+CLDSPS*SALFAZ
      CLDSP =CLDSPS*CALFAZ-CNDSPS*SALFAZ
C
C  Z-TRANSFORM SETUP
C
      GN1(1) =TI4/TI2-1.
      FR1(1) =1./TI2
C
      GN1(2) =1./TI1
      FR1(2) =1./TI1
C
      GN1(3) =1./TE3
      FR1(3) =1./TE3
C
      GN1(4) =1./TE1
      FR1(4) =1./TE1
C
```

```
      GN1(5) =1./TE4
      FR1(5) =1./TE4
C
      GN1(6) =1./TED1
      FR1(6) =1./TED1
C
      GN1(7) =TEN2/TED2=1.
      FR1(7) =1./TED2
C
      GN1(8) =-XKPP/TC1
      FR1(8) =1./TC1
C
      GN1(9) =XKQQ*TCN1/TCD1
      FR1(9) =1./TCD1
C
      GN1(10)=XKQQ/TCD1
      FR1(10)=1./TCD1
C
      GN1(11)=XKQ2*(1.-TCN2/TCD21)/(TCD21-TCD22)
      FR1(11)=1./TCD21
C
      GN1(12)=XKQ2*(TCN2/TCD22-1.)/(TCD21-TCD22)
      FR1(12)=1./TCD22
C
      GN1(13)=XKRR
      FR1(13)=1./TCN3
C
      GN1(14)=XKRN/TC2
      FR1(14)=1./TC2
C
      GN1(15)=1./TIDA
      FR1(15)=1./TIDA
C
      GN1(16)=1./TIDB
      FR1(16)=1./TIDB
C
      GN1(17)=1./TIDM
      FR1(17)=1./TIDM
C
      GN2(1) =WNSP*WNSP
      A2ND(1)=2.*ZSP*WNSP
      B2ND(1)=WNSP*WNSP
C
      GN2(2) =WNA*WNA
      A2ND(2)=2.*ZA*WNA
      B2ND(2)=WNA*WNA
C
      GN2(3) =WNE*WNE
      A2ND(3)=2.*ZE*WNE
      B2ND(3)=WNE*WNE
C
      GN2(4) =WNR*WNR
      A2ND(4)=2.*ZR*WNR
      B2ND(4)=WNR*WNR
C
C
      CALL ZXFORM(NUM1,GN1,FR1,Z01,Z11,NUM2,IRR,GN2,A2ND,B2ND,
     1            Z021,Z022,Z121,Z122,DT)
C
      RETURN
C
      END
```

```
C       TITLE                                   LOOP1
        SUBROUTINE LOOP1
C
        COMMON /BLK1 / IMODE    ,IDT      ,ITIMES   ,DT       ,NDT
       1,     TIME     ,D2R      ,ID
C
        COMMON /BLK2 / UB       ,VB       ,WB       ,PB       ,QB
       1,     RB       ,PHIR     ,THETR    ,PSIR     ,PHI      ,THET
       2,     PSI      ,DM       ,BETA     ,ALFA     ,BETAR    ,ALFAR
       3,     ALT      ,ANY      ,ANZ      ,CLB      ,CLDA     ,CLDR
       4,     CLDBP    ,CLDSP    ,CLRR     ,CLPR     ,CNP      ,CNDA
       5,     CNDR     ,CNDBP    ,CNDSP    ,CNPR     ,CYPR     ,DELTAA
       6,     DELTAE   ,DELTAP   ,G2Z      ,G7Z      ,PSZ      ,PT2Z
       7,     DSP(2)   ,DBP(2)   ,PT2S(2)  ,PL4(2)   ,AJC(2)   ,RPMM(2)
       8,     T(2)     ,WEC1(2)  ,DQSAR
C
        COMMON /BLK3 / CDZ      ,CDA1     ,CDA2     ,CLZ      ,CLA1
       1,     CMZ      ,CMA1     ,CMA2     ,CDDE     ,CDDBP    ,CDDSP
       2,     CLFDE    ,CLFDBP   ,CLFDSP   ,CLFDB    ,GBARZ    ,VZ
       3,     AREA     ,XMASS    ,CHORD    ,SPAN     ,G        ,XXT
       4,     XZT      ,XLT      ,XMT      ,XNT      ,XIXX     ,XIYY
       5,     XIZZ     ,XIXZ     ,CYB      ,CYDP     ,CYPB     ,CLAB
       6,     CMAD     ,CMDR     ,CMDE     ,CMDBP    ,CLBS     ,CLPBS
       7,     CLRBS    ,CLDAS    ,CLDRS    ,CLDBPS   ,CLDSPS   ,CNBS
       8,     CNPBS    ,CNRBS    ,CNDAS    ,CNDRS    ,CNDBPS   ,CNDSPS
C
        COMMON /BLK5 / XKPP     ,XK00     ,XK02     ,XKBR     ,XKRN
       1,     TC1      ,TC2      ,TCN1     ,TCD1     ,TCN2     ,TCD21
       2,     TCD22    ,TCN3     ,WNA      ,ZA       ,WNE      ,ZE
       3,     WNR      ,ZR       ,TI1      ,TI2      ,TI4      ,WNSP
       4,     ZSP      ,TE1      ,TC3      ,TC4      ,TE11     ,TEN2
       5,     TED2     ,TIDA     ,TID3     ,TICH
C
        COMMON / BLK7 / G1A     ,G1B      ,G1C      ,G1D      ,G2A
       1,     G2B      ,G2C      ,G2E      ,G2F      ,G2G      ,G2H
       2,     G2I      ,G2J      ,G2K      ,G2L      ,G3A      ,G3B
       3,     G4A      ,G4B      ,G4C      ,G4D      ,G4E      ,G4F
       4,     G5A      ,G5B      ,G5C      ,G6A      ,G7A      ,G7B
       5,     G7C      ,G7D      ,G8A      ,G8B      ,G8C      ,G8D
       6,     G8E      ,G8F      ,G8G      ,G8H      ,G8I      ,G8J
       7,     G8K      ,G8L
C
        COMMON /BLK8 / G9A      ,G9B      ,G9C      ,G9D      ,G9E
       1,     G9F      ,G10A     ,G11A     ,G11B     ,G11C     ,G11D
       2,     G11E     ,G11F     ,G11G     ,G12A     ,G12B     ,G14A
       3,     G14B     ,G14C     ,G14D     ,G14E     ,G14F     ,G15A
       4,     G15B     ,G15C     ,G15D     ,G16A     ,G16B     ,G16C
       5,     G16D     ,G16E     ,G16F     ,G16G     ,G16H     ,G17A
       6,     G17B     ,G17C     ,G18A     ,G1AB     ,G19C
       7,     G19A     ,G19B     ,G20A     ,G20B
C
        COMMON /BLK10/ GN1(17)  ,FR1(17)  ,ZD1(17)  ,ZI1(17)  ,GN2(4)
       1,     A2ND(4)  ,B2ND(4)  ,Z021(4)  ,Z022(4)  ,ZI21(4)  ,ZI22(4)
C
        COMMON /BLK11/ ALFAZ    ,ALFAZR   ,DSPZ     ,WICZ     ,DBPZ
       1,     THETZ    ,DEZ      ,PBIC     ,QBIC     ,RBIC     ,PHIIC
       2,     THEIC    ,PSIIC    ,DMIC     ,BETAIC   ,ALFAIC   ,ALTIC
       3,     ICDSP(2) ,DSPIC(2) ,DSPDIC(2),ICDBP(2) ,DBPIC(2) ,DBPDIC(2)
       4,     ICRPM(2) ,RPMIC(2) ,ICAJ(2)  ,AJIC(2)  ,AJDIC(2) ,AJCDIC(2)
       5,     ICWFAB(2),WFABIC(2),ICWFBR(2),WFBRIC(2),ICPSAS   ,PSASIC
       6,     PSADIC   ,ICQSAS   ,QSASIC   ,ICRSAS   ,RSASIC   ,RSADIC
       7,     RSAIIC   ,RSAZIC   ,ICDA     ,DAIC     ,DADIC    ,ICDR
       8,     DRIC     ,DRDIC    ,XB       ,DEIC     ,DEDIC    ,ZB
       9,     ZB       ,XMB      ,ALTZ
C
C
C
        DIMENSION RAMPLA(2),SLOPLA(2),PLALMT(2),IPLA(2),IWORD8(2)
C
        DATA SLOPLA/0.,0./,PLALMT/0.,0./,IPLA/0,0/
C
C
C
C  INPUT SIGNALS
C
        DO 10 I=1,2
        RAMPLA(I)=SLOPLA(I)*TIME
        IF (RAMPLA(I).GT.PLALMT(I)) RAMPLA(I)=PLALMT(I)
        PLA(I)   =IPLA(I)*RAMPLA(I)
```

```
78            RPMM(I)   =0.0
79            AJC(I)    =0.0
80         10 CONTINUE
81      C
82            CALL INLET
83      C
84            CALL ENGINE
85      C
86            CALL CONTRL
87      C
88            CALL AIRFRM
89      C
90            CALL XFERDA(IMODE,IWORDS,0)
91      C
92            IF (IMODE.GT.0) TIME=TIME+DT
93      C
94            RETURN
95      C
96            END
```

```
C      TITLE                                    INLET
       SUBROUTINE INLET
C
       COMMON /BLK1 / IMODE     ,IDT      ,ITIMES   ,DT       ,NDT
      1,     TIME      ,D2R      ,ID
C
       COMMON /BLK2 / UB        ,VB       ,WB       ,PB       ,QB
      1,     RB        ,PHIR     ,THETR    ,PSIR     ,PHI      ,THET
      2,     PSI       ,DM       ,BETA     ,ALFA     ,BETAR    ,ALFAR
      3,     ALT       ,ANY      ,ANZ      ,CLR      ,CLDA     ,CLDR
      4,     CLDBR     ,CLDSP    ,CLRB     ,CLPB     ,CNR      ,CNDA
      5,     CNDR      ,CNDBR    ,CNDSP    ,CNRB     ,CNPB     ,DELTAA
      6,     DELTAE    ,DELTAR   ,GGZ      ,G7Z      ,PS7      ,PT27
      7,     DSP(2)    ,DBP(2)   ,PT23(2)  ,PLA(2)   ,AJC(2)   ,RPMM(2)
      8,     T(2)      ,WEC1(2)  ,DORAR
C
       COMMON /BLK5 / XKPP      ,XKQQ     ,XKQ2     ,XKRR     ,XKRN
      1,     TC1       ,TC2      ,TCN1     ,TCD1     ,TCN2     ,TCD21
      2,     TCD22     ,TCN3     ,WNA      ,ZA       ,WNE      ,ZE
      3,     WNR       ,ZR       ,TI1      ,TI2      ,TI4      ,WISP
      4,     ZSP       ,TE1      ,TE3      ,TE4      ,TEC1     ,TCN2
      5,     TCD2      ,TIDA     ,TIDB     ,TIDM
C
       COMMON /BLK6 / XKI5      ,XKI6     ,XKI10    ,XKI12    ,XKI15
      1,     XKI16     ,XKI19    ,XKI20    ,XKI23
C
       COMMON / BLK7 / G1A      ,G1B      ,G1C      ,G1F      ,G2A
      1,     G2B       ,G2C      ,G2E      ,G2F      ,G2G      ,G2H
      2,     G2I       ,G2J      ,G2K      ,G2L      ,G3A      ,G3B
      3,     G4A       ,G4B      ,G4C      ,G4D      ,G4E      ,G4F
      4,     G5A       ,G5B      ,G5C      ,G6A      ,G7A      ,G7B
      5,     G7C       ,G7D      ,G8A      ,G8B      ,G8C      ,G8D
      6,     G8E       ,G8F      ,G8G      ,G8H      ,G6I      ,G8J
      7,     G8K       ,G8L
C
       COMMON /BLK8 / G9A       ,G9B      ,G9C      ,G9D      ,G9E
      1,     G9F       ,G10A     ,G11A     ,G11B     ,G11C     ,G11D
      2,     G11E      ,G11F     ,G11G     ,G12A     ,G12B     ,G14A
      3,     G14B      ,G14C     ,G14D     ,G14E     ,G14F     ,G15A
      4,     G15B      ,G15C     ,G15D     ,G16A     ,G16B     ,G16C
      5,     G16D      ,G16E     ,G16F     ,G16G     ,G16H     ,G17A
      6,     G17B      ,G17C     ,G18A     ,G18B     ,G18C
      7,     G19A      ,G19B     ,G20A     ,G20B
C
       COMMON /BLK10/ GN1(17)   ,FR1(17)  ,ZO1(17)  ,ZI1(17)  ,GN2(4)
      1,     A2ND(4)   ,B2ND(4)  ,ZO2I(4)  ,ZO22(4)  ,ZI2I(4)  ,ZI22(4)
C
       COMMON /BLK11/ ALFAZ     ,ALFAZR   ,DSPZ     ,WICZ     ,DBPZ
      1,     THETZ     ,DEZ      ,PBIC     ,QBIC     ,RBIC     ,PHIIC
      2,     THEIC     ,PSIIC    ,DMIC     ,BETAIC   ,ALFAIC   ,ALTIC
      3,     ICDSP(2)  ,DSPIC(2) ,DSPDIC(2),ICDBP(2) ,DBPIC(2) ,DBPDIC(2)
      4,     ICRPM(2)  ,RPMIC(2) ,ICAJ(2)  ,AJIC(2)  ,AJDIC(2) ,AJCDIC(2)
      5,     ICWFAB(2),WFABIC(2),ICWFPB(2),WFPBIC(2),ICRSAS   ,PSASIC
      6,     PSADIC    ,ICQSAS   ,QSASIC   ,ICRSAS   ,RSASIC   ,RSADIC
      7,     RSAIIC    ,RSA2IC   ,ICDA     ,DAIC     ,DADIC    ,ICDE
      8,     DEIC      ,DEDIC    ,ICDR     ,DRIC     ,DRDIC    ,XR
      9,     ZB        ,XMB      ,ALTZ
C
C
C
       DIMENSION DSPI(2),DSPIP(2),DSPIPP(2),DSPIS(2),DSPISP(2)
      1,DOUT(2),DOUTP(2),DOUTPP(2),PSO(2),PS(2),DE(2)
      2,XSD(2),DBP1(2),DBP2(2),DBPR(2)
      3,DWI(2),DWIP(2),DWIC(2),DW(2)
      4,PT2(2),G1(2),G4(2),G5(2),G8(2),G9(2),G10(2),G11(2),G13(2),G14(2)
      5,G15(2),G16(2),G17(2),G1A(2),DG10(2),DWICO(2),DWC(2),WEC(2)
C
C
       ALFAT=ZO1(15)*ALFAT+ZI1(15)*ALFA
C
       BETAT=ZO1(16)*BETAT+ZI1(16)*BETA
C
       DMT=ZO1(17)*DMT+ZI1(17)*DM
C
       DG1=ABS(ANZ)-G3B
       IF (DG1.LT.0.0) DG1=0.0
       G3=G3A*DG1
       G6=G6A*DG1
```

```
      C
            G12=(G12A+G12B*ALFA)*ALFA
      C
            DG5=ALFAT*ALFAZ
      C
            DG2=ABS(DG5*G7A)
            DG3=DG2*DG2
            DG4=DG2*DG3
            G7=G7B*DG4+G7C*DG3+G7D*DG2+G7Z
      C
            DG6=DG5*DG5
            DG7=DG5*DG6
            G2=G2A*DG7+G2B*DG6+G2C*DG5+G2Z+(G2E*DG7+G2F*DG6+G2G*DG5+G2H
           1   +(G2I*DG7+G2J*DG6+G2K*DG5+G2L)*DMT)*DMT
      C
            G19=(G19A+G19B*DM)*DM
      C
            DG8=(G1A+ABS(BETAT)+G1B)*BETAT*BETAT
            DG9=(G1C*ABS(BETAT)+G1D)*BETAT*BETAT
            IF (BETAT) 100,101,101
        100 G1(1)=DG8
            G1(2)=DG9
            GO TO 102
        101 G1(1)=DG9
            G1(2)=DG8
        102 CONTINUE
      C
            DG10(1)=BETA
            DG10(2)=-BETA
            DG11=BETA*BETA
            DG12=ALFA*ALFA
      C
            PT3=XKI23*DQBAR
            WEC2=XKI20*DM
      C
            DO 1000 I=1,2
      C
            DSPIS(I) =G6+G7+XKI19*DMT+XKI12*G1(I)
            DSPI(I)  =.5*(3.*DSPIS(I)-DSPISP(I))
            DSPISP(I)=DSPIS(I)
      C
            IF (IMODE) 201,2,202
        201 IF (IQDSP(I).EQ.0) GO TO 202
      C
            DSP(I)   =DSPIC(I)
            DOUTP(I) =DSP(I)-DSPZ
            DOUTPP(I)=DOUTP(I)=DSPDIC(I)*DT
            GO TO 203
      C
        202 DOUT(I)=Z021(I)*DOUTP(I)+Z022(I)*DOUTPP(I)+ZI21(I)*DSPI(I)
           1        +ZI22(I)*DSPIP(I)
      C
            DSP(I)=DOUT(I)+DSPZ
      C
            DOUTPP(I)=DOUTP(I)
            DOUTP(I) =DOUT(I)
      C
        203 DSPIP(I)=DSPI(I)
      C
            WEC(I)=WEC1(I)+WEC2
            DWI(I) =XKI5*DBP(I)+WEC(I)
            DWIP(I)=.5*(3.*DWI(I)-DWIP(I))
      C
            DW(I)=Z01(2)*DW(I)+ZI1(2)*DWIP(I)
            DWIP(I)=DWI(I)
      C
            DWIC(I)=DW(I)+WICZ
      C
            DSC(I)=G2-XKI10*G1(I)-G3
      C
            G4(I)=(G4A+G4B*DSP(I)+G4C*DWIC(I))*ALFA
           1     +(G4D+G4E*DSP(I)+G4F*DWIC(I))*DG12
      C
            G5(I)=(G5A+G5B*DSP(I)+G5C*DWIC(I))*DM
      C
            G8(I)=(G8A+G8B*DSP(I))*DG10(I)+(G8C+G8D*DSP(I))*DG11
           1     +((G8E+G8F*DSP(I))*DG10(I)+(G8G+G8H*DSP(I))*DG11+((G8I+
           2     G8J*DSP(I))*DG10(I)+(G8K+G8L*DSP(I))*DG11)*DWIC(I))*DWIC(I)
```

```
156     C
157           G9(I)=G9A+G9B*DSP(I)+(G9C+G9D*DSP(I)+(G9E+G9F*DSP(I))*DWIC(I))
158          1      *DWIC(I)
159     C
160           PS(I)=G4(I)+G5(I)+G8(I)+G9(I)
161     C
162           DE(I)=PS(I)+PSZ-PSC(I)
163     C
164           X5D(I)=XKI6*DE(I)
165     C
166           IF (IMODE) 211,2,212
167       211 IF (ICDBP(I).EQ.0) GO TO 212
168     C
169           DBP(I) =DBPIC(I)
170           DBP2(I)=TI4*X5D(I)-TI2*DBPDIC(I)
171           DBP1(I)=DBP(I)-DBP2(I)
172           GO TO 213
173     C
174       212 DBP1(I)=DBP1(I)+X5D(I)*DT
175           DBP2(I)=ZB1(I)*DBP2(I)+ZI1(I)*X5D(I)
176     C
177           DBP(I)=DBP1(I)+DBP2(I)
178     C
179       213 DBPR(I)=(DBP(I)+DBPZ)*17.4
180     C
181           G14(I)=(G14A+G14B*DSP(I)+G14C*DWIC(I))*ALFA
182          1      +(G14D+G14E*DSP(I)+G14F*DWIC(I))*DG12
183     C
184           G15(I)=G15A+G15B*DSP(I)+(G15C+G15D*DSP(I))*DWIC(I)
185     C
186           G16(I)=(G16A+G16B*DSP(I))*DG10(I)+(G16C+G16D*DSP(I))*DG11+((G16E
187          1      +G16F*DSP(I))*DG10(I)+(G16G+G16H*DSP(I))*DG11)*DWIC(I)
188     C
189           G17(I)=(G17A+G17B*DSP(I)+G17C*DWIC(I))*DM
190     C
191           PT2(I)=G14(I)+G15(I)+G16(I)+G17(I)
192     C
193           PT2S(I)=PT3+PT2(I)+PT2Z+G19
194     C
195           G10(I)=DSP(I)+G10A*DM
196           G20=(G20A+G20B*ALFA)*ALFA
197     C
198           IF (DG10(I)) 110,112,112
199       110 IF(G11G*DG11-G10(I)+G11E*G20) 111,111,115
200       111 G11(I)=G11A+G11F*DG11
201           GO TO 114
202       112 IF(G11D*DG11-G10(I)+G11E*G20) 113,113,115
203       113 G11(I)=G11A
204       114 DG13=G10(I)-G11B
205           IF (DG13.GE.0.0) G11(I)=G11(I)+G11C*DG13
206     C
207           G13(I)=XKI16*DSP(I)*DM
208           DWICU(I)=G11(I)+G12+G13(I)-XKI15*DM
209           DWC(I)=DWIC(I)-DWICU(I)
210           IF (DWC(I)) 115,115,116
211       115 G18(I)=0.0
212           GO TO 1000
213       116 G18(I)=G18A+DWC(I)+G18B*SIN(G18C*DWC(I))
214     C
215      1000 CONTINUE
216     C
217          2 RETURN
218     C
219           END
```

```
C       TITLE                                   ENGINE
        SUBROUTINE ENGINE
C
        COMMON /BLK1 / IMODE    ,IDT      ,ITIMES   ,DT       ,NDT
       1,     TIME     ,D2R      ,ID
C
        COMMON /BLK2 / UB       ,VB       ,WB       ,PB       ,QB
       1,     RB       ,PHIR     ,THETR    ,PSIR     ,PHI      ,THET
       2,     PSI      ,DN       ,BETA     ,ALFA     ,BETAR    ,ALFAR
       3,     ALT      ,ANY      ,ANZ      ,CLP      ,CLDA     ,CLDR
       4,     CLDBP    ,CLDSP    ,CLRB     ,CLPB     ,CNR      ,CNDA
       5,     CNDR     ,CNDBP    ,CNDSP    ,CNRB     ,CNPB     ,DELTAA
       6,     DELTAE   ,DELTAR   ,G2Y      ,G2Z      ,PSZ      ,PT2Z
       7,     DSP(2)   ,DBP(2)   ,PT2S(2)  ,PLA(2)   ,AJS(2)   ,RPMM(2)
       8,     T(2)     ,WEC1(2)  ,DQBAR
C
        COMMON /BLK5 / XKPP     ,XKQQ     ,XKQ2     ,XKRR     ,XKRN
       1,     TC1      ,TC2      ,TCN1     ,TCD1     ,TCN2     ,TCD21
       2,     TCD22    ,TCN3     ,WNA      ,ZA       ,WNF      ,ZF
       3,     WNR      ,ZR       ,TI1      ,TI2      ,TI4      ,WNSP
       4,     ZSP      ,TE1      ,TE3      ,TE4      ,TED1     ,TEN2
       5,     TCD2     ,TIDA     ,TID3     ,TIDM
C
        COMMON /BLK9 / XKE3     ,XKE4     ,XKE7     ,XKE8     ,XKE9
       1,     XKE10    ,XKE11    ,XKE12    ,XKE13    ,XKE14    ,XKE15
       2,     XKE16    ,XKE17    ,XKE18    ,XKE19    ,XKE20
C
        COMMON /BLK10/ GN1(17)  ,FR1(17)  ,Z01(17)  ,ZI1(17)  ,GN2(4)
       1,     A2ND(4)  ,B2ND(4)  ,Z021(4)  ,Z022(4)  ,ZI21(4)  ,ZI22(4)
C
        COMMON /BLK11/ ALFAZ    ,ALFAZR   ,DSPZ     ,WICZ     ,D3PZ
       1,     THETZ    ,DEZ      ,PBIC     ,QBIC     ,RBIC     ,PHIIC
       2,     THEIC    ,PSIIC    ,DMIC     ,BETAIC   ,ALFAIC   ,ALTIC
       3,     ICDSP(2) ,DSPIC(2) ,DSPDIC(2),ICDBP(2) ,DBPIC(2) ,DBPDIC(2)
       4,     ICRPM(2) ,RPMIC(2) ,ICAJ(2)  ,AJIC(2)  ,AJDIC(2) ,AJCDIC(2)
       5,     ICWFAB(2),WFABIC(2),ICWFBI(2),WFBIC(2),ICRSAS   ,RSASIC
       6,     RSADIC   ,ICRSAS   ,RSASIC   ,ICRSAS   ,RSASIC   ,RSADIC
       7,     RSA1IC   ,RSA2IC   ,ICDA     ,DAIC     ,DADIC    ,ICDE
       8,     DEIC     ,DEDIC    ,ICDR     ,DRIC     ,DRDIC    ,XB
       9,     ZB       ,XMB      ,ALTZ
C
C
        DIMENSION PT4I(2),PT4IP(2),PT4(2),PT4P(2),PLAP(2),RPMI(2),RPMIP(2)
       1,RPM(2),RPMP(2),RPMMP(2),AJ(2),AJI(2),AJBUT(2),AJI(2),AJ2(2)
       2,WFPB(2),WFPBI(2),WFPBIP(2),WFAB(2),WFABI(2)
C
C
        DO 1000 I=1,2
        PT4I(I) = XKE18*PT2S(I)+XKE13*RPM(I)
        PT4IP(I)=.5*(3.*PT4I(I)-PT4IP(I))
C
        PT4(I)=Z01(5)*PT4(I)+ZI1(5)*PT4IP(I)
C
        PT4IP(I)=PT4I(I)
C
        RPMI(I)=XKE9*WFPB(I)+XKE11*AJ(I)-XKE12*WFAB(I)-XKE8*PT2S(I)
        RPMIP(I)=.5*(3.*RPMI(I)-RPMIP(I))
C
        IF (IMODE) 1,2000,2
      1 IF (ICRPM(I).EQ.0) GO TO 2
C
        RPM(I)=RPMIC(I)
        GO TO 3
C
      2 RPM(I)=Z01(4)*RPM(I)+ZI1(4)*RPMIP(I)
C
      3 RPMIP(I)=RPMI(I)
C
        WEC1(I)=XKE4*RPM(I)
C
        RPMP(I) =.5*(RPMP(I)+RPM(I))
        RPMMP(I)=.5*(3.*RPMM(I)-RPMMP(I))
C
        AJI(I)=XKE3*(RPMMP(I)-RPMP(I))
C
        RPMP(I) =RPM(I)
        RPMMP(I)=RPMM(I)
```

```
      C
            IF (IMODE) 11,2000,12
         11 IF (ICAJ(I).EQ.0) GO TO 12
      C
            AJ(I)   =AJIC(I)
            AJOUT(I)=AJ(I)-AJC(I)
            AJ2(I)  =TEN2*AJI(I)-TED2*(AJDIC(I)-AJCDIC(I))
            AJ1(I)  =AJOUT(I)-AJ2(I)
            GO TO 13
      C
         12 AJ1(I)  =AJ1(I)+AJI(I)*DT
            AJ2(I)  =ZO1(7)*AJ2(I)+ZI1(7)*AJI(I)
            AJOUT(I)=AJ1(I)+AJ2(I)
      C
            AJ(I)=AJOUT(I)+AJC(I)
      C
         13 WFPBI(I) =XKE15*PT4(I)-XKE14*PPM(I)
            WFPBIP(I)=.5*(WFPBI(I)+WFPPI?(I))
      C
            IF (IMODE) 21,2000,22
         21 IF (ICWFPB(I).EQ.0) GO TO 22
      C
            WFPB(I)=WFPBIC(I)
            GO TO 23
      C
         22 WFPB(I)=ZO1(6)*WFPB(I)+ZI1(6)*WFPBIP(I)
      C
         23 WFPBIP(I)=WFPBI(I)
      C
            PLAP(I)=.5*(3.*PLA(I)-PLAP(I))
            PT4P(I)=.5*(PT4(I)+PT4P(I))
      C
            WFABI(I)=XKE17*PLAP(I)+XKE19*PT4P(I)
      C
            PLAP(I)=PLA(I)
            PT4P(I)=PT4(I)
      C
            IF (IMODE) 31,2000,32
         31 IF (ICWFAB(I).EQ.0) GO TO 32
      C
            WFAB(I)=WFABIC(I)
            GO TO 33
      C
         32 WFAB(I)=ZO1(3)*WFAB(I)+ZI1(3)*WFABI(I)
      C
         33 T(I)=XKE16*WFAB(I)-XKE7*AJ(I)+XKE20*PT4(I)+XKE10*WFPB(I)
      C
       1000 CONTINUE
      C
       2000 RETURN
      C
            END
```

```
C      TITLE                                          CONTRL
       SUBROUTINE CONTRL
C
       COMMON /BLK1 / IMODE     ,IDT       ,ITIMES    ,DT        ,NDT
      1,     TIME      ,D2R       ,ID
C
       COMMON /BLK2 / UB        ,VB        ,WB        ,PB        ,QB
      1,     RB        ,PHIR      ,THETR     ,PSIR      ,PHI       ,THET
      2,     PSI       ,DM        ,BETA      ,ALFA      ,BETAR     ,ALFAR
      3,     ALT       ,ANY       ,ANZ       ,CLB       ,CLTA      ,CLDR
      4,     CLDBP     ,CLDSP     ,CLRB      ,CLPB      ,CNB       ,CNDA
      5,     CNDR      ,CNDBP     ,CNDSP     ,CNRB      ,CNPB      ,DELTAA
      6,     DELTAE    ,DELTAR    ,G2Z       ,G77       ,PS7       ,PT2Z
      7,     DSP(2)    ,DBP(2)    ,PT2S(2)   ,PLA(2)    ,AJC(2)    ,RPMM(2)
      8,     T(2)      ,WEC1(2)   ,DQBAR
C
       COMMON /BLK4 / PSASU     ,PSASL     ,QSASU     ,QSASL     ,QBIU
      1,     QBIL      ,RSASU     ,RSASL
C
       COMMON /BLK10/ GN1(17)   ,FF1(17)   ,Z01(17)   ,Z11(17)   ,GN2(4)
      1,     A2ND(4)   ,92ND(4)   ,Z021(4)   ,Z022(4)   ,Z121(4)   ,Z122(4)
C
       COMMON /BLK11/ ALFAZ     ,ALFAZP    ,DSPZ      ,WIGZ      ,DBPZ
      1,     THETZ     ,DEZ       ,PBIC      ,QBIC      ,RBIC      ,PHIIC
      2,     THEIC     ,PSIIC     ,DNIC      ,BETAIC    ,ALFAIC    ,ALTIC
      3,     ICDSP(2)  ,DSPIC(2)  ,DSPDIC(2),ICDBP(2)  ,DBPIC(2)  ,DBPDIC(2)
      4,     ICRPM(2)  ,RPMIC(2)  ,ICAJ(2)   ,AJIC(2)   ,AJDIC(2)  ,AJCDIC(2)
      5,     ICWFAB(2),WFABIC(2),ICWFBS(2),WFBBIC(2),ICPSAS    ,PSASIC
      6,     PSADIC    ,ICQSAS    ,QSASIC    ,ICRSAS    ,RSASIC    ,PSADIC
      7,     RSAIIC    ,RSA2IC    ,ICDA      ,DAIC      ,DADIC     ,ICDE
      8,     DEIC      ,DEDIC     ,ICDR      ,DRIC      ,DRDIC     ,X7
      9,     ZB        ,XMB       ,ALT7
C
C*** NOTE ***
C
C  REFER TO ROUTINE UTILTY FOR EXPLANATION OF VALLMT
C
C***
C
C  ROLL SAS
C
        PBDEG =PB/D2R
        PBDEGP=.5*(3.*PBDEG-PBDEGP)
C
        IF (IMODE) 1,100,2
      1 IF (ICPSAS.EQ.0) GO TO 2
C
        PSAS=PSASIC
        POUT=PSAS
        GO TO 3
C
      2 POUT=Z01(6)*POUT+Z11(6)*PBDEGP
C
        PSAS=VALLMT(POUT,PSASU,PSASL)
C
      3 PBDEGP=PBDEG
C
C  PITCH SAS  ( NO IC PROVIDED )
C
        QBDEG =QB/D2R
        QB12I =.5*(3.*QBDEG-QBDEGP)
        QBDEGP=QBDEG
        QB34I =VALLMT(QB12I,QBIU,QBIL)
C
        QOUT1 =Z01(9)*QOUT1+GN1(9)*(QB12I-QB12IP)
        QB12IP=QB12I
C
        QOUT2 =Z01(10)*QOUT2+Z11(10)*QB12I
C
        QOUT3 =Z01(11)*QOUT3+Z11(11)*QB34I
C
        QOUT4 =Z01(12)*QOUT4+Z11(12)*QB34I
C
        QOUT=QOUT1+QOUT2+QOUT3+QOUT4
C
        QSAS=VALLMT(QOUT,QSASU,QSASL)
C
```

```
C  YAW SAS
C
      RBDEG =RP/D2R
      RBI   =.5*(3.*RBDEG-RBDEGP)
      RBDEGP=RBDEG
C
      ANYP=.5*(3.*ANY-ANYP)
C
      IF (IMODE) 21,100,22
   21 IF (ICRSAS.EQ.0) GO TO 22
C
      RSAS =RSA1IC+RSA2IC
      ROUT1=RSA1IC
      ROUT2=RSA2IC
      GO TO 23
C
   22 ROUT1=ZO1(13)*ROUT1+GN1(13)*(RBI-RBIP)
      ROUT2=ZO1(14)*ROUT2+ZI1(14)*ANYP
      ROUT =ROUT1+ROUT2
C
      RSAS=VALLMT(ROUT,PSASU,PSASL)
C
   23 RBIP=RBI
      ANYP=ANY
C
C  AILERON ANGLE
C
      DAI  =.5*(PSASP+PSAS)
      PSASP=PSAS
C
      IF (IMODE) 31,100,32
   31 IF (ICDA.EQ.0) GO TO 32
C
      DELTAA=DAIC
      DAOPP =DELTAA-DADIC*DT
      DAIP  =PSAS-PSADIC*DT
      GO TO 33
C
   32 DELTAA=ZO21(2)*DAOP+ZO22(2)*DAOPP+ZI21(2)*DAI+ZI22(2)*DAIP
C
      DAOPP=DAOP
      DAIP =DAI
C
   33 DAOP=DELTAA
C
C  ELEVATOR ANGLE
C
      DEI  =.5*(QSASP+QSAS)
      QSASP=QSAS
C
      IF (IMODE) 41,100,42
   41 IF (ICDE.EQ.0) GO TO 42
C
      DELTAE=DEIC
      DEOPP =DELTAE-DEDIC*DT
      GO TO 43
C
   42 DELTAE=ZO21(3)*DEOP+ZO22(3)*DEOPP+ZI21(3)*DEI+ZI22(3)*DEIP
C
      DEOPP=DEOP
C
   43 DEOP=DELTAE
      DEIP=DEI
C
      DETL=DELTAE+DEZ
C
C  RUDDER ANGLE
C
      DRI  =.5*(RSASP+RSAS)
      RSASP=RSAS
C
      IF (IMODE) 51,100,52
   51 IF (ICDR.EQ.0) GO TO 52
C
      DELTAR=DRIC
      DROPP =DELTAR-DRDIC*DT
      DRIP  =RSAS-RSADIC*DT
      GO TO 53
```

```
C
   52 DELTAR=Z021(4)*DR0P+Z022(4)*DP0PP+ZI21(4)*DRI+ZI22(4)*DRIP
C
      DR0PP=DR0P
      DRIP =DRI
C
   53 DR0P=DELTAR
C
  100 RETURN
C
      END
```

```
C       TITLE                                          AIRFRM
        SUBROUTINE AIRFRM
C
        COMMON /BLK1 / IMODE     ,IDT       ,ITIMES    ,DT        ,NDT
       1,     TIME      ,D2R       ,ID
C
        COMMON /BLK2 / UB        ,VB        ,WB        ,PB        ,QB
       1,     RB        ,PHIR      ,THETB     ,PSIR      ,PHI       ,THET
       2,     PSI       ,DM        ,BETA      ,ALFA      ,BETAB     ,ALFAB
       3,     ALT       ,ANY       ,ANZ       ,CLB       ,CLDA      ,CLDB
       4,     CLDBB     ,CLDSB     ,CLBB      ,CLBB      ,CNB       ,CNDA
       5,     CNBB      ,CNDBB     ,CNDSB     ,CNBB      ,CNBB      ,DELTAA
       6,     DELTAE    ,DELTAR    ,G2Z       ,G77       ,PST       ,PT2Z
       7,     DSP(2)    ,DBP(2)    ,PT2S(2)   ,PLA(2)    ,AJC(2)    ,RPMM(2)
       8,     T(2)      ,WEC1(2)   ,DBBAR
C
        COMMON /BLK3 / CDZ       ,CDA1      ,CDA2      ,CLZ       ,CLA1
       1,     CMZ       ,CMA1      ,CMA2      ,CDDE      ,CDDBP     ,CDDSP
       2,     CLFDE     ,CLFDBP    ,CLFDSP    ,CLFCB     ,QBARZ     ,VZ
       3,     AREA      ,XMASS     ,CHORD     ,SPAN      ,G         ,XXT
       4,     XZT       ,XLT       ,XNT       ,XNT       ,XIXX      ,XIYY
       5,     XIZZ      ,XIXZ      ,CYB       ,CYBB      ,CYBB      ,CLAP
       6,     CMAD      ,CMDB      ,CMDE      ,CMDBP     ,CLBS      ,CLPBS
       7,     CLRBS     ,CLDAS     ,CLDBS     ,CLDBPS    ,CLBSPS    ,CNBS
       8,     CNPBS     ,CNRBS     ,CNDAS     ,CNDBS     ,CNDBPS    ,CNDSPS
C
        COMMON /BLK11/ ALFAZ     ,ALFAZB    ,DSPZ      ,WICZ      ,DBPZ
       1,     THETZ     ,DEZ       ,PBIC      ,QBIC      ,RBIC      ,PHIIC
       2,     THEIC     ,PSIIC     ,DNIC      ,BETAIC    ,ALFAIC    ,ALTIC
       3,     ICDSP(2)  ,DSPIC(2)  ,DSPZIC(2) ,ICDBP(2)  ,DBPIC(2)  ,DBPDIC(2)
       4,     ICRPM(2)  ,RPMIC(2)  ,ICAJ(2)   ,AJIC(2)   ,AJZIC(2)  ,AJCDIC(2)
       5,     ICWFAB(2),WFABIC(2),ICWFBD(2),WFBDIC(2),ICBSAS    ,BSASIC
       6,     PSABIC    ,ICQSAS    ,QSASIC    ,ICPSAS    ,RSASIC    ,PSADIC
       7,     PSAIIC    ,RSADIC    ,ICDA      ,DAIC      ,DADIC     ,ICDE
       8,     DEIC      ,DEDIC     ,ICDB      ,DBIC      ,DBDIC     ,XB
       9,     ZB        ,XMB       ,ALTZ
C
C
        DIMENSION BUFFER(60)
C
        DATA NVAR/10/,INTORD/2/
C
C
        IF (IMODE) 1,100,2
C
C  INTEGRATION ROUTINE SETUP
C
      1 CALL MGRATE(NVAR,DT,BUFFER,INTORD,TIME,ERROR)
C
C
        CALL ARDC62(ALTZ,SPDSND,RHO)
        QBARZ =.5*RHO*VZ*VZ
C
        QUAN1 =QBARZ*AREA/XMASS
        QUAN2 =ALFAZR*VZ
        QUAN3 =SPAN/(2.*VZ)
        QUAN4 =QBARZ*QUAN3
        QUAN5 =AREA*SPAN/XIXX
        QUAN6 =AREA*SPAN/XIZZ
        QUAN7 =AREA*CHORD/XIYY
        QUAN8 =CHORD/(2.*VZ)
        QUAN9 =QBARZ*QUAN8
        QUAN10=QUAN9/VZ
        QUAN11=XIXZ/XIXX
        QUAN12=XIXZ/XIZZ
        QUAN13=1.-QUAN11*QUAN12
        QUAN14=2.*DSPZ
C
        ALFA2 =ALFAZR*ALFAZR
        CDAZ  =CDZ+CDA1*ALFAZR+CDA2*ALFA2
        CLAZ  =CLZ+CLA1*ALFAZR
        CMAZ  =CMZ+CMA1*ALFAZR+CMA2*ALFA2
        XZ=QUAN1*CDAZ-QUAN1*CLAZ*ALFAZR
        ZZ=QUAN1*CLAZ+QUAN1*CDAZ*ALFAZR
        QUAN17=QBARZ*CMAZ
C
        GO TO 3
```

```
C
C  INTEGRATION
C
    2 CALL GRATBN(BUFFER,UBD,UB,VBD,VB,WBD,WB,PBD,PB,QQD,QB,RBD,RB
     1,            PHID,PHIR,THED,THETR,PSID,PSIR,ALTD,ALT)
C
C
      PHI  =PHIR/D2R
      THET =THETR/D2R
      PSI  =PSIR/D2R
C
      DH= UB/968.
      BETAR=VB/VZ
      BETA =BETAR/D2R
      ALFAR=WB/VZ
      ALFA =ALFAR/D2R
C
C
    3 SPHI  =SIN(PHIR)
      THETTL=THET7+THET
      DELALT=ALT-ALTZ
C
      CALL ARDC62(ALT,SPDSND,RHO)
      QBAR  =.5*RHO*(VZ+UB)**2
      DQBAR =QBAR-QBARZ
C
      AWRPR =ALFAZR+ALFAR
C
      QUAN15=QBAR*AREA/XMASS
      AWRPR2=AWRPR*AWRPR
C
      CDA=CDZ+CDA1*AWRPR+CDA2*AWRPR2
      CLA=CLZ+CLA1*AWRPR
      CMA=CMZ+CMA1*AWRPR+CMA2*AWRPR2
C
C  SYMMETRIC QUANTITIES
C
      DBPS=DBP(1)+DBP(2)
      DSPS=DSP(1)+DSP(2)-QUAN14
      TS  =T(1)+T(2)
C
C  ASYMMETRIC QUANTITIES
C
      DBPA=DBP(1)-DBP(2)
      DSPA=DSP(1)-DSP(2)
      TA  =T(1)-T(2)
C
C  DRAG AND LIFT IN WIND AXES
C
      DRAG =QUAN15*(CDA+CDDE*DELTAE+CDDBP*DBPS+CDDSP*DSPS)
      XLIFT=QUAN15*(CLA+CLFDE*DELTAE+CLFDBP*DBPS+CLFDSP*DSPS
     1               +QUAN8*CLFQB*QB)
C
C  ACCELERATIONS IN BODY AXES
C
      A1=XZ+XB-DRAG+XLIFT*AWRPR
      A2=QUAN1*(CYB*BETA+CYDR*DELTAR+QUAN3*CYRB*RB)
      A3=ZZ+ZB-DRAG*AWRPR-XLIFT
      A4=QUAN8*(QBAR*(CLB*BETA+CLAB*ALFA+PETA+CLDA*DELTAA+CLDR*DELTAR
     1          +CLDBP*DBPA+CLDSP*DSPA)+QUAN4*(CLRP*RP+CLPR*PR))
      A6=QUAN6*(QBAR*(CNB*BETA+CNDA*DELTAA+CNDE*DELTAE+CNDBP*DBPA
     1          +CNDSP*DSPA)+QUAN4*(CNRB*RB+CNPR*PB))
      QUAN16=A6+XNT*TA
      QUAN18=-VZ*RB+G*SPHI+QUAN2*PB
C
      UBD=A1-QUAN2*QB-G*THETR+XXT*TS
      VBD=A2+QUAN18
      WBD=A3+VZ*QB+XZT*TS
C
      AS =QUAN7*(QUAN10*CMAD*WBD+QUAN9*CMQB*QB-QUAN17+QBAR*(CMA
     1          +CMDE*DELTAE+CMDBP*DBPS))+XMD
C
      PBD=(A4+QUAN11*QUAN16+XLT*TA)/QUAN13
      QBD=A5+XMT*TS
      RBD=QUAN12*PBD+QUAN16
C
C  ANGLE RATES OF CHANGE
C
```

```
156           PHID=P3
157           THED=Q3
158           PSID=R3
159     C
160     C  ALTITUDE RATE
161     C
162           ALTD=VZ*THETTL*D2R-VB*PHIP-WB+QUAN2
163     C
164     C  NY AND NZ PER G
165     C
166           ANY=(VBD-QUAN18+44.*RBD)/G
167     C
168           ANZ=(WBD-VZ+QB)/G
169     C
170       100 RETURN
171     C
172           END
```

REFERENCES

1. Anon.: U. S. Standard Atmosphere, 1962. Available from Superintendent of Documents, U. S. Government Printing Office, Washington, D. C.

2. Ralston, Anthony: A First Course in Numerical Analysis. McGraw Hill, N. Y., 1965.

3. Neuman, Frank; and Foster, John D.: Investigation of a Digital Automatic Aircraft Landing System in Turbulence. NASA TN D-6066, 1970.

TABLE 1.— LIMITS FOR INLET PRESSURE FUNCTIONS

$$f\left(w_{i_c},\ \delta_{sp},\ X\right) = \sum_{i=0}^{i_{max}} \sum_{j=0}^{j_{max}} \sum_{k=1}^{k_{max}} C_{ijk} w_{i_c}^{i}\, \delta_{sp}^{j} X^{k}$$

Pressure Functions	i_{max}	j_{max}	k_{max}
$f_a\left(w_{i_c},\ \delta_{sp}\right)$	1	1	---
$f_b\left(w_{i_c},\ \delta_{sp}\right)$	2	1	---
$f_a\left(w_{i_c},\ \delta_{sp},\ \alpha\right)$	1	1	2
$f_b\left(w_{i_c},\ \delta_{sp},\ \alpha\right)$	1	1	2
$f_a\left(w_{i_c},\ \delta_{sp},\ \beta\right)$	1	1	2
$f_b\left(w_{i_c},\ \delta_{sp},\ \beta\right)$	2	1	2
$f_a\left(w_{i_c},\ M\right)$	1	---	1
$f_b\left(w_{i_c},\ M\right)$	1	---	1

TABLE 2.— LIST OF FORTRAN QUANTITIES

Airframe			
Quantity	Fortran	Units	Description
$\dot{u}$	UBD	m/sec^2	Forward acceleration
$\dot{v}$	VBD	m/sec^2	Right acceleration
$\dot{w}$	WBD	m/sec^2	Vertical acceleration
u	UB	m/sec^2	Forward velocity
v	VB	m/sec^2	Lateral velocity
w	WB	m/sec^2	Vertical velocity
$\dot{p}$	PBD	rad/sec^2	Roll angular acceleration
$\dot{q}$	QBD	rad/sec^2	Pitch angular acceleration
$\dot{r}$	RBD	rad/sec^2	Yaw angular acceleration
p	PB	rad/sec	Roll angular velocity
q	QB	rad/sec	Pitch angular velocity
r	RB	rad/sec	Yaw angular velocity
p(o)	PBIC	deg/sec	Roll angular velocity, I.C.
q(o)	QBIC	deg/sec	Pitch angular velocity, I.C.
r(o)	RBIC	deg/sec	Yaw angular velocity, I.C.
$\dot{\phi}$	PHID	rad/sec	Roll rate
$\dot{\theta}$	THED	rad/sec	Pitch rate
$\dot{\psi}$	PSID	rad/sec	Yaw rate
ϕ	PHIR	rad	Roll angle
$\Delta\theta$	THETR	rad	Pitch angle
ψ	PSIR	rad	Yaw angle
ϕ	PHI	deg	Roll angle
$\Delta\theta$	THET	deg	Pitch angle
ψ	PSI	deg	Yaw angle
θ_o	THETZ	deg	Pitch angle, reference condition
θ	THETTL	deg	Total pitch angle
sin ϕ	SPHI	ND	Sine of roll angle
$\phi(o)$	PHIIC	deg	Roll angle, I.C.
$\Delta\theta(o)$	THEIC	deg	Pitch angle, I.C.
$\psi(o)$	PSIIC	deg	Yaw angle, I.C.

TABLE 2.– LIST OF FORTRAN QUANTITIES - Continued

Airframe			
Quantity	Fortran	Units	Description
ΔM	DM	ND	Mach number increment
$\Delta M(o)$	DMIC	ND	Mach number increment, I.C.
β	BETA	deg	Sideslip angle
α	ALFA	deg	Angle of attack
β	BETAR	rad	Sideslip angle
α	ALFAR	rad	Angle of attack
$\beta(o)$	BETAIC	deg	Sideslip angle, I.C.
$\alpha(o)$	ALFAIC	deg	Angle of attack, I.C.
α_{w_o}	ALFAZ	deg	Angle of attack, reference condition
α_{w_o}	ALFAZR	rad	Angle of attack, ref. condition
$\dot{h}$	ALTD	m/sec	Altitude rate
h	ALT	m	Altitude
h(o)	ALTIC	m	Altitude, I.C.
$\pi/180$	D2R	rad/deg	Conversion factor, degrees to radians
δ_{bp_s}	DBPS	cm	Symmetric inlet bypass actuator pos.
δ_{sp_s}	DSPS	cm	Symmetric inlet spike position
δ_{t_s}	TS	ND	Incremental symmetric engine thrust
δ_{bp_a}	DBPA	cm	Antisymmetric inlet bypass actuator position
δ_{sp_a}	DSPA	cm	Antisymmetric inlet spike position
δ_{t_a}	TA	ND	Antisymmetric engine thrust
$C_D(\alpha)$	CDA	ND	Drag coefficient
$C_L(\alpha)$	CLA	ND	Lift coefficient
$C_m(\alpha)$	CMA	ND	Pitching moment coefficient
$C_D(o)$	CDAZ	ND	Drag coefficient, I.C.
$C_L(o)$	CLAZ	ND	Lift coefficient, I.C.
$C_m(o)$	CMAZ	ND	Pitching moment coefficient, I.C.

TABLE 2.— LIST OF FORTRAN QUANTITIES - Continued

Airframe			
Quantity	Fortran	Units	Description
C_{D_f}	CDZ	ND	Zero order term in $C_D(\alpha)$
C_{D_α}	CDA1	1/rad	First order term in $C_D(\alpha)$
$C_{D_{\alpha^2}}$	CDA2	$1/rad^2$	Second order term in $C_D(\alpha)$
C_{L_f}	CLZ	ND	Zero order term in $C_L(\alpha)$
C_{L_α}	CLA1	1/rad	First order term in $C_L(\alpha)$
C_{m_f}	CMZ	ND	Zero order term in $C_m(\alpha)$
C_{m_α}	CMA1	1/rad	First order term in $C_m(\alpha)$
$C_{m_{\alpha^2}}$	CMA2	$1/rad^2$	Second order term in $C_m(\alpha)$
D/m	DRAG	m/sec^2	Drag in stability axes
L/m	XLIFT	m/sec^2	Lift in stability axes
$C_{D_{\delta_e}}$	CDDE	1/deg	Aerodynamic derivative
$C_{D_{\delta_{bp}}}$	CDDBP	1/cm	Aerodynamic derivative
$C_{D_{\delta_{sp}}}$	CDDSP	1/cm	Aerodynamic derivative
$C_{L_{\delta_e}}$	CLFDE	1/deg	Aerodynamic derivative
$C_{L_{\delta_{bp}}}$	CLFDBP	1/cm	Aerodynamic derivative
$C_{L_{\delta_{sp}}}$	CLFDSP	1/cm	Aerodynamic derivative
C_{L_q}	CLFQB	1/rad	Aerodynamic derivative
q_v	QBAR	N/m^2	Dynamic pressure
Δq_v	DQBAR	N/m^2	$\Delta q_v = q_v - q_{v_o}$
q_{v_o}	QBARZ	N/m^2	Dynamic pressure, reference cond.
V	VZ	m/sec	Initial forward velocity
S	AREA	m^2	Wing area
m	XMASS	kg	Mass of vehicle
c	CHORD	m	Mean aerodynamic chord

TABLE 2.— LIST OF FORTRAN QUANTITIES - Continued

Airframe			
Quantity	Fortran	Units	Description
b	SPAN	m	Wing span
ρ	RHO	kg/m^3	Air density
g	G	m/sec^2	Acceleration due to gravity
X_o	XZ	m/sec^2	Forward acceleration calculated for ref. cond.
Z_o	ZZ	m/sec^2	Downward acceleration calculated for ref. cond.
X_b	XB	m/sec^2	Biased quantity for forward acceleration
Z_b	ZB	m/sec^2	Biased quantity for downward acceleration
M_b	XMB	rad/sec^2	Biased quantity for pitching angular acceleration
X_{δ_t}	XXT	m/sec^2	Forward acceleration due to thrust
Z_{δ_t}	XZT	m/sec^2	Downward accel. due to thrust
L_{δ_t}	XLT	rad/sec^2	Rolling acceleration due to thrust
M_{δ_t}	XMT	rad/sec^2	Pitching acceleration due to thrust
N_{δ_t}	XNT	rad/sec^2	Yawing acceleration due to thrust
I_{xx}	XIXX	$kg\ m^2$	Rolling moment of inertia
I_{yy}	XIYY	$kg\ m^2$	Pitching moment of inertia
I_{zz}	XIZZ	$kg\ m^2$	Yawing moment of inertia
I_{xz}	XIXZ	$kg\ m^2$	Product of inertia
C_{y_β}	CYB	1/deg	Aerodynamic derivative
$C_{y_{\delta_r}}$	CYDR	1/deg	Aerodynamic derivative
C_{y_r}	CYRB	1/rad	Aerodynamic derivative
C_{ℓ_β}	CLB	1/deg	Aerodynamic derivative
$C_{\ell_{\alpha\beta}}$	CLAB	$1/deg^2$	Aerodynamic derivative
$C_{\ell_{\delta_a}}$	CLDA	1/deg	Aerodynamic derivative

TABLE 2.— LIST OF FORTRAN QUANTITIES - Continued

Airframe			
Quantity	Fortran	Units	Description
$C_{\ell_{\delta_r}}$	CLDR	1/deg	Aerodynamic derivative
$C_{\ell_{\delta_{bp}}}$	CLDBP	1/cm	Aerodynamic derivative
$C_{\ell_{\delta_{sp}}}$	CLDSP	1/cm	Aerodynamic derivative
C_{ℓ_r}	CLRB	1/rad	Aerodynamic derivative
C_{ℓ_p}	CLPB	1/rad	Aerodynamic derivative
$C_{m_{\dot{\alpha}}}$	CMAD	1/rad	Aerodynamic derivative
C_{m_q}	CMQB	1/rad	Aerodynamic derivative
$C_{m_{\delta_e}}$	CMDE	1/deg	Aerodynamic derivative
$C_{m_{\delta_{bp}}}$	CMDBP	1/cm	Aerodynamic derivative
C_{n_β}	CNB	1/deg	Aerodynamic derivative
$C_{n_{\delta_a}}$	CNDA	1/deg	Aerodynamic derivative
$C_{n_{\delta_r}}$	CNDR	1/deg	Aerodynamic derivative
$C_{n_{\delta_{bp}}}$	CNDBP	1/cm	Aerodynamic derivative
$C_{n_{\delta_{sp}}}$	CNDSP	1/cm	Aerodynamic derivative
C_{n_r}	CNRB	1/rad	Aerodynamic derivative
C_{n_p}	CNPB	1/rad	Aerodynamic derivative
C_{ℓ_β}	CLBS	1/deg	Aerodynamic derivative
$C^s_{\ell_p}$	CLPBS	1/rad	Aerodynamic derivative
$C^s_{\ell_r}$	CLRBS	1/rad	Aerodynamic derivative
$C^s_{\ell_{\delta_a}}$	CLDAS	1/deg	Aerodynamic derivative
$C^s_{\ell_{\delta_r}}$	CLDRS	1/deg	Aerodynamic derivative
$C^s_{\ell_{\delta_{bp}}}$	CLDBPS	1/cm	Aerodynamic derivative

TABLE 2.— LIST OF FORTRAN QUANTITIES - Continued

Airframe			
Quantity	Fortran	Units	Description
$C^s_{\ell_{\delta_{sp}}}$	CLDSPS	1/cm	Aerodynamic derivative
$C^s_{n_\beta}$	CNBS	1/deg	Aerodynamic derivative
$C^s_{n_p}$	CNPBS	1/rad	Aerodynamic derivative
$C^s_{n_r}$	CNRBS	1/rad	Aerodynamic derivative
$C^s_{n_{\delta_a}}$	CNDAS	1/deg	Aerodynamic derivative
$C^s_{n_{\delta_r}}$	CNDRS	1/deg	Aerodynamic derivative
$C^s_{n_{\delta_{bp}}}$	CNDBPS	1/cm	Aerodynamic derivative
$C^s_{n_{\delta_{sp}}}$	CNDSPS	1/cm	Aerodynamic derivative
$\cos \alpha_{w_o}$	CALFAZ	ND	
$\sin \alpha_{w_o}$	SALFAZ	ND	
$\cos^2 \alpha_{w_o}$	CALFZ2	ND	
$\sin^2 \alpha_{w_o}$	SALFZ2	ND	
n_z	ANZ	g	Normal acceleration
	DT	sec	Frame time
SAS Control			
p_{sas}	PSAS	deg	Roll SAS
q_{sas}	QSAS	deg	Pitch SAS
r_{sas}	RSAS	deg	Yaw SAS
δ_a	DELTAA	deg	Aileron angle
$\Delta\delta_e$	DELTAE	deg	Elevator angle
δ_r	DELTAR	deg	Rudder angle
δ_e	DETL	deg	Total elevator angle
k_{pp}	XKPP	sec	SAS gain
p_{sas} (U.L.)	PSASU	deg	p_{sas} upper limit
p_{sas} (L.L.)	PSASL	deg	p_{sas} lower limit

TABLE 2.— LIST OF FORTRAN QUANTITIES - Continued

SAS Control			
Quantity	Fortran	Units	Description
k_{qq}	XKQQ	sec	SAS gain
k_{q2}	XKQ2	sec	SAS gain
q_{sas} (U.L.)	QSASU	deg	Total q_{sas} upper limit
q_{sas} (L.L.)	QSASL	deg	Total q_{sas} lower limit
q_{sas_ℓ} (U.L.)	QBIU	deg	Lagged q_{sas} upper limit
q_{sas_ℓ} (L.L.)	QBILL	deg	Lagged q_{sas} lower limit
k_{rr}	XKRR	sec	SAS gain
k_{rn}	XKRN	deg/g	SAS gain
n_{y_n}	ANY	g	Lateral acceleration at nose
r_{sas} (U.L.)	RSASU	deg	r_{sas} upper limit
r_{sas} (L.L.)	RSASL	deg	r_{sas} lower limit
T_{p1}	TC1	sec	Time constant
T_{r2}	TC2	sec	Time constant
T_{q2}	TCN1	sec	Time constant
T_{q1}	TCD1	sec	Time constant
T_{q5}	TCN2	sec	Time constant
T_{q3}	TCD21	sec	Time constant
T_{q4}	TCD22	sec	Time constant
T_{r1}	TCN3	sec	Time constant
p	PBDEG	deg/sec	Roll angular velocity
q	QBDEG	deg/sec	Pitch angular velocity
r	RBDEG	deg/sec	Yaw angular velocity
w_{n_a}	WNA	rad/sec	Undamped natural frequency for aileron servo
ρ_a	ZA	ND	Damping ratio of aileron servo
w_{n_e}	WNE	rad/sec	Undamped natural frequency for elevon servo
ρ_e	ZE	ND	Damping ratio of elevon servo
w_{n_r}	WNR	rad/sec	Undamped natural frequency for rudder servo
ρ_r	ZR	ND	Damping ratio of rudder servo

TABLE 2.– LIST OF FORTRAN QUANTITIES - Continued

SAS Control			
Quantity	Fortran	Units	Description
$p_{sas}(o)$	PSASIC	deg/sec	I.C. for p_{sas}
$q_{sas}(o)$	QSASIC	deg/sec	I.C. for q_{sas}
$\delta_a(o)$	DAIC	deg	I.C. for aileron
$\delta_e(o)$	DBIC	deg	I.C. for elevon
$\delta_r(o)$	DRIC	deg	I.C. for rudder
$\delta_e(o)$	DEZ	deg	Reference condition for elevon
$\dot{p}_{sas}(o)$	PSADIC	deg/sec^2	I.C. for p_{sas} rate
$\dot{r}_{sas}(o)$	PSADIC	deg/sec^2	I.C. for r_{sas} rate
$\dot{\delta}_a(o)$	DADIC	deg/sec	I.C. for aileron rate
$\dot{\delta}_e(o)$	DEDIC	deg/sec	I.C. for elevon rate
$\dot{\delta}_r(o)$	DRDIC	deg/sec	I.C. for rudder rate
$r_{sas_1}(o)$	RSAIIC	deg	I.C. for first part of r_{sas} equation
$r_{sas_2}(o)$	RSA2IC	deg	I.C. for second part of r_{sas} equation
Inlet			
ΔM_m	DMT	ND	Measured increment of Mach number
α_m	ALFAT	deg	Measured angle of attack
β_m	BETAT	deg	Measured sideslip angle
δ_{sp_o}	DSPZ	cm	Reference condition for inlet spike
$w_{i_{c_o}}$	WICZ	lb/sec	Ref. condition for inlet airflow
$\left(p_s/p_{t_m}\right)_o$	PSZ	ND	Compensation for signal pressure at reference condition
$\left(p_t/p_{t_o}\right)_o$	PT2Z	ND	Compensation for pressure recovery at reference condition
$\left(p_s/p_{t_m}\right)_c$	PSC	ND	Command signal for bypass control
δ_{sp}	DSP	cm	Inlet spike position
p_s/p_{t_o}	PS	ND	Bypass signal pressure
$\Delta\delta_{bp}$	DBP	cm	Bypass actuator position
δ_{bp}	DBPR	cm	Total bypass actuator position

TABLE 2.— LIST OF FORTRAN QUANTITIES - Continued

Inlet			
Quantity	Fortran	Units	Description
δ_{bp_o}	DBPZ	cm	Ref. condition for bypass actuator
Δw_{i_c}	DWIC	kg/sec	Inlet airflow
p_{t_2}/p_{t_o}	PT2	ND	Inlet pressure recovery
$\Delta\left(p_{t_2}/p_{t_o}\right)$	PT2S	ND	Incremental pressure recovery
$f(\beta_m)$	G1	ND	Spike & bypass command function
$f_{bp}(\alpha_m, M_m)$	G2	ND	Bypass command function
$f_{bp}(n_{z_m})$	G3	ND	Bypass command function
$f_b(w_{i_c}, \delta_{sp}, \alpha)$	G4	ND	Signal pressure function
$f_b(w_{i_c}, M)$	G5	ND	Signal pressure function
$f_{sp}(n_{z_m})$	G6	in.	Spike command function
$f_{sp}(\alpha_m)$	G7	in.	Spike command function
$f_b(w_{i_c}, \delta_{sp}, \beta)$	G8	ND	Signal pressure function
$f_b(w_{i_c}, \delta_{sp})$	G9	ND	Signal pressure function
δ_{sp_d}	G10	in.	Unstart boundary function
$f_{c_a}(\delta_{sp_d})+f_{c_a}(\beta)$	G11	kg/sec	Unstart boundary function
$f_{c_a}(\alpha)$	G12	kg/sec	Unstart boundary function
$f_{c_a}(\delta_{sp}, M)+k_{i_{15}}\Delta M$	G13	kg/sec	Unstart boundary function
$f_a(w_{i_c}, \delta_{sp}, \alpha)$	G14	ND	Pressure recovery function
$f_a(w_{i_c}, \delta_{sp})$	G15	ND	Pressure recovery function
$f_a(w_{i_c}, \delta_{sp}, \beta)$	G16	ND	Pressure recovery function
$f_a(w_{i_c}, M)$	G17	ND	Pressure recovery function
$f_d(w_{i_c})$	G18	cm-sec/kg	Shockwave position function
$f_1(M)$	G19	ND	Incremental press. recovery function
$f_{c_s}(\alpha)$	G20	in.	Unstart boundary function
T_{i_1}	TI1	sec	Time constant
T_{i_2}	TI2	sec	Time constant
T_{i_4}	TI4	sec	Time constant
k_{i_5}	XKI5	kg/cm-sec	Bypass loop gain
k_{i_6}	XKI6	cm	Bypass loop gain

TABLE 2.— LIST OF FORTRAN QUANTITIES - Continued

Inlet			
Quantity	Fortran	Units	Description
$k_{i_{10}}$	XKI10	ND	Bypass command gain
$k_{i_{12}}$	XKI12	cm	Spike command gain
$k_{i_{15}}$	XKI15	kg/sec	Unstart function gain
$k_{i_{16}}$	XKI16	kg/cm-sec	Unstart function gain
$k_{i_{19}}$	XKI19	cm	Spike gain
$k_{i_{20}}$	XKI20	kg/sec	Engine airflow gain
$k_{i_{23}}$	XKI23	ND	Incremental pressure recovery gain
$w_{n_{sp}}$	WNSP	rad/sec	Undamped natural freq. of spike servo
ρ_{sp}	ZSP	ND	Damping ratio of spike servo
T_M	TIDM	sec	Time constant
T_β	TIDB	sec	Time constant
T_α	TIDA	sec	Time constant
$f_{bp}(\alpha_{w_o}, 0)$	G2Z	ND	Ref. cond. for bypass command function
$f_{sp}(\alpha_{w_o})$	G7Z	cm	Ref. cond. for spike command function
	ICDSP	ND	I.C. mode control for z-transform integration
	ICDBP	ND	I.C. mode control for z-transform integration
$\delta_{sp}(o)$	DSPIC	cm	I.C. for spike position
$\dot{\delta}_{sp}(o)$	DSPDIC	cm/sec	I.C. for spike position rate
$\delta_{bp}(o)$	DBPIC	cm	I.C. for bypass position
$\dot{\delta}_{bp}(o)$	DBPDIC	cm/sec	I.C. for bypass position rate
Engine			
PLA	PLA	deg	Power level angle
A_{j_c}	AJC	cm^2	Command signal for exhaust nozzle area
N	RPMM	%	Command incremental engine rotor speed
N_m	RPM	%	Incremental engine rotor speed
Pt_4/Pt_o	PT4	ND	Primary burner pressure ratio

TABLE 2.— LIST OF FORTRAN QUANTITIES - Continued

Engine			
Quantity	Fortran	Units	Description
w_{fpb}	WFPB	%	Incremental primary burner fuel flow rate
w_{fab}	WFAB	%	Incremental afterburner fuel flow rate
A_j	AJ	cm^2	Incremental exhaust nozzle area
δ_t	T	%	Incremental thrust
w_{e_c}	WEC	kg/sec	Incremental airflow demanded by engine
T_{e1}	TE1	sec	Time constant
T_{e3}	TE3	sec	Time constant
T_{e4}	TE4	sec	Time constant
T_{ed1}	TED1	sec	Time constant
T_{en2}	TEN2	sec	Time constant
T_{ed2}	TED2	sec	Time constant
K_{e3}	XKE3	$cm^2/\%N$	Gain
K_{e4}	XKE4	$(kg/sec)/\%N$	Gain
K_{e7}	XKE7	$\%\delta_t/cm^2$	Gain
K_{e8}	XKE8	ND	Gain
K_{e9}	XKE9	ND	Gain
K_{e10}	XKE10	$\%\delta_t/\%w_{fpb}$	Gain
K_{e11}	XKE11	$1/cm^2$	Gain
K_{e12}	XKE12	ND	Gain
K_{e13}	XKE13	$1/\%N$	Gain
K_{e14}	XKE14	$\%w_{fpb}/\%N$	Gain
K_{e15}	XKE15	$\%w_{fpb}$	Gain
K_{e16}	XKE16	$\%\delta_t/\%w_{fab}$	Gain
K_{e17}	XKE17	$\%w_{fab}/deg$	Gain
K_{e18}	XKE18	ND	Gain
K_{e19}	XKE19	$\%w_{fab}$	Gain
K_{e20}	XKE20	$\%\delta_t$	Gain
	ICRPM	ND	I.C. mode control for z-transform integration
N(0)	RPMIC	%N	I.C. for engine rotor speed

TABLE 2.– LIST OF FORTRAN QUANTITIES - Concluded

Engine			
Quantity	Fortran	Units	Description
	ICAJ	ND	I.C. mode control for z-transform integration
$A_j(0)$	AJIC	cm^2	I.C. for exhaust nozzle area
$\dot{A}_j(0)$	AJDIC	cm^2/sec	I.C. for exhaust nozzle area rate
	AJCDIC	cm^2/sec	I.C. for command exh. noz. area rate
	ICWFPB	ND	I.C. mode control for z-transform integration
$w_{fpb}(0)$	WFPBIC	$\%w_{fpb}$	I.C. for primary burner fuel flow
	ICWFAB	ND	I.C. mode control for z-transform integration
	WFABIC	$\%w_{fab}$	I.C. for afterburner fuel flow

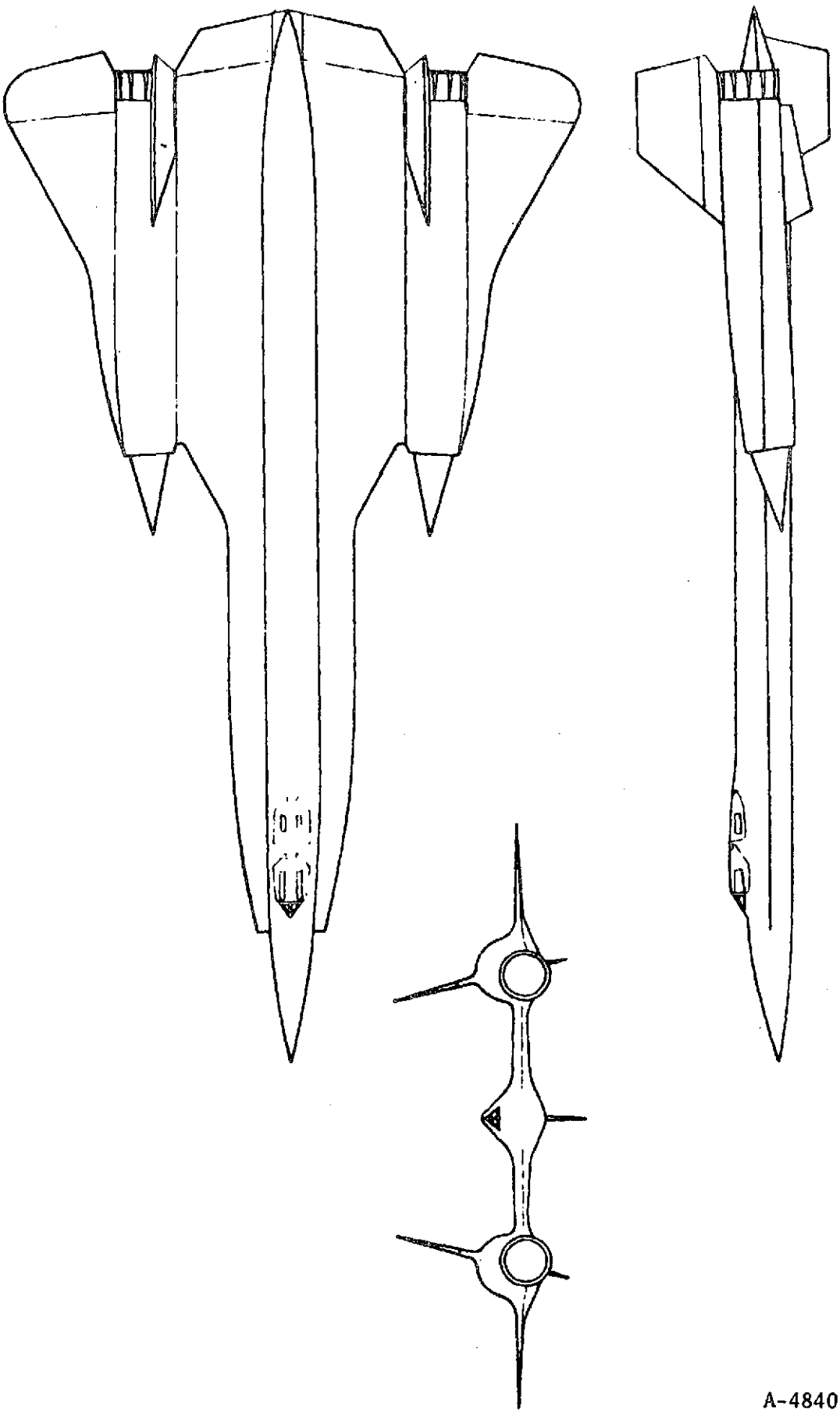

Figure 1.— Three-view drawing of the aircraft.

A-4840

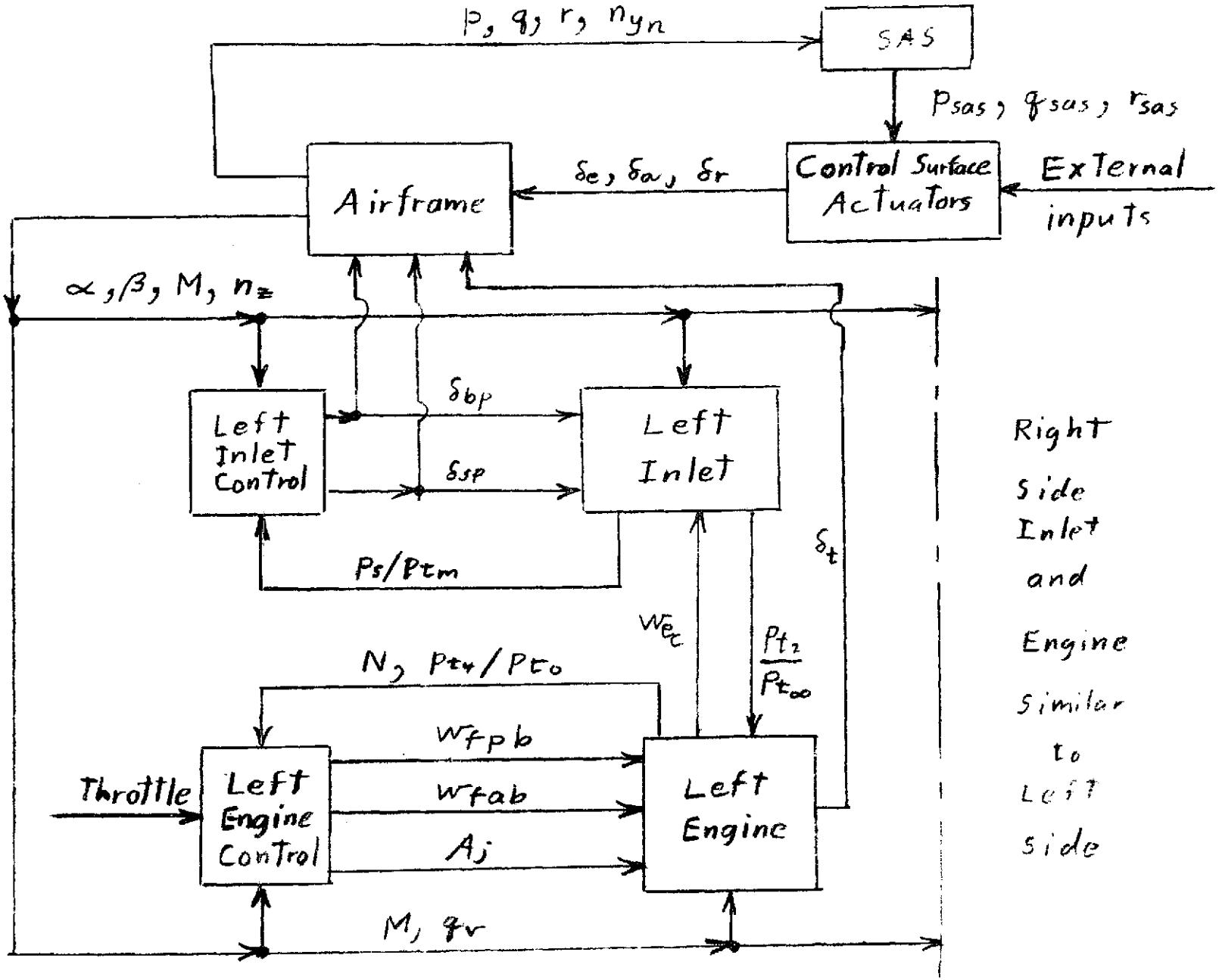

Figure 2.– Representation of aircraft propulsion system.

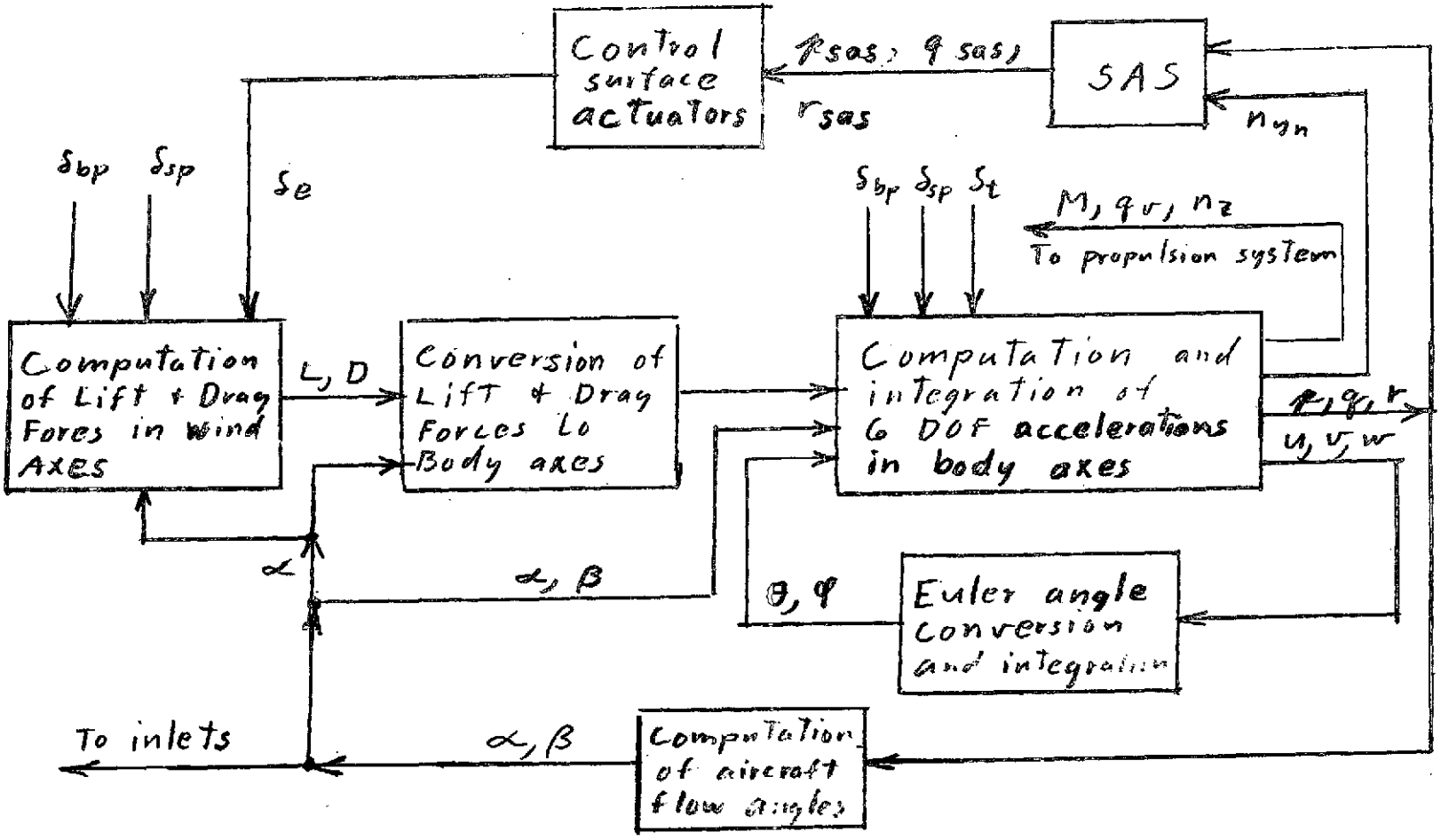

Figure 3.— Airframe simulation.

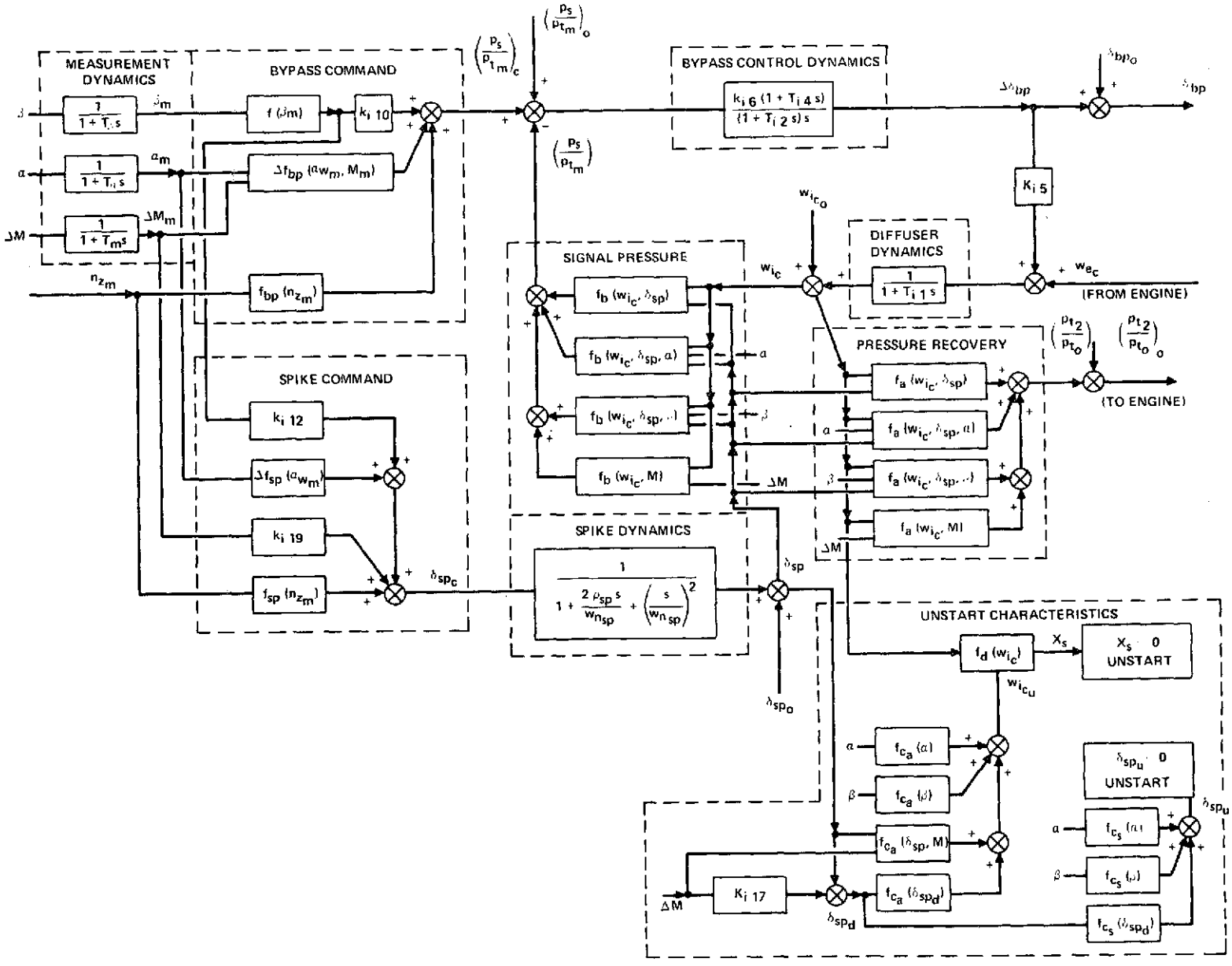

Figure 4.— Inlet block diagram.

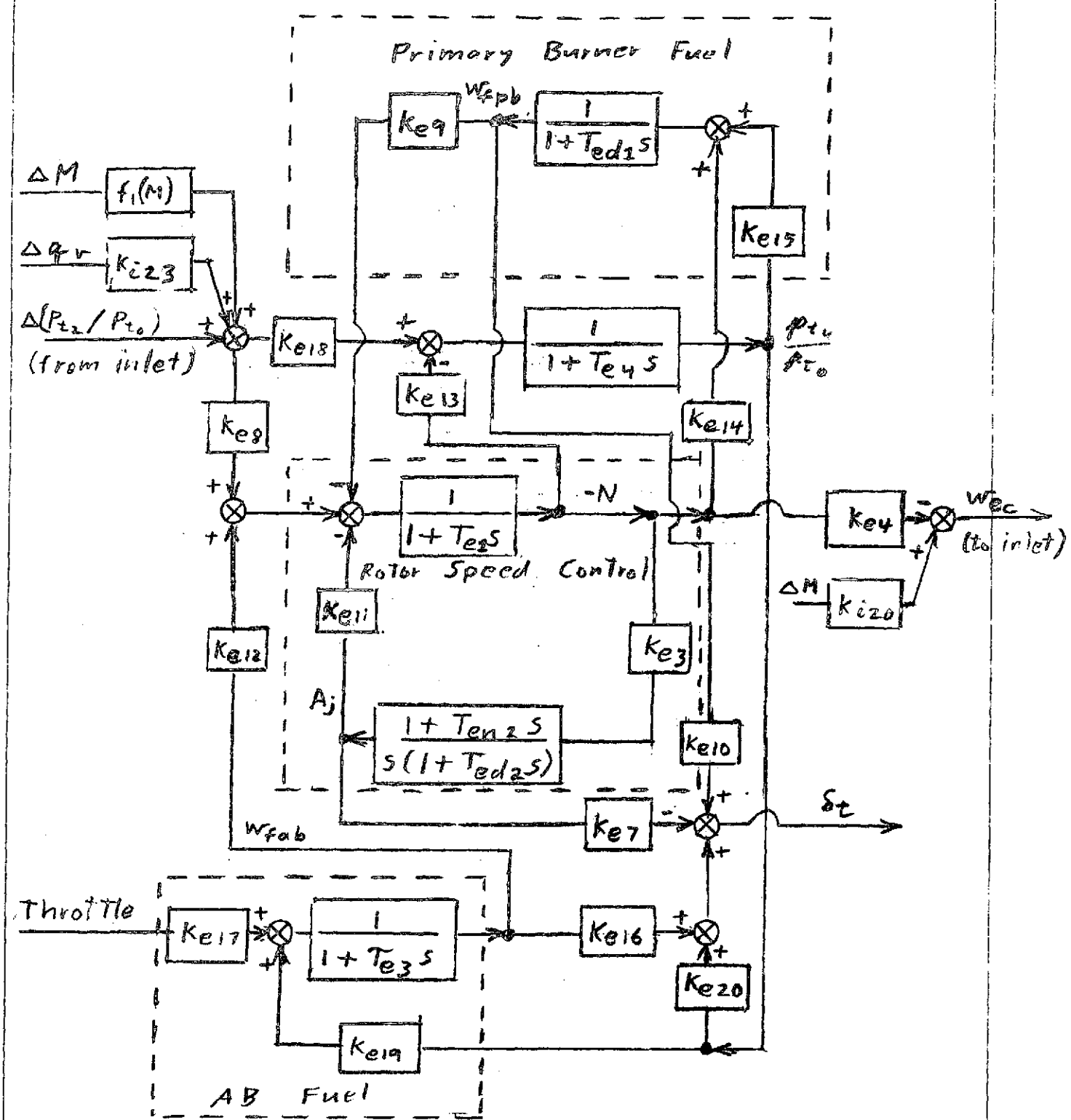

Figure 5.— Engine block diagram.